Surface Charge Behavior and Adsorption of Surfactants on Carbonate Rocks

by

Alfonso Rodriguez

A Thesis Presented to the

FACULTY OF THE COLLEGE OF GRADUATE STUDIES

KING FAHD UNIVERSITY OF PETROLEUM & MINERALS

DHAHRAN, SAUDI ARABIA

In Partial Fulfillment of the
Requirements for the Degree of

MASTER OF SCIENCE

In

PETROLEUM ENGINEERING

October, 1992

Order Number 1354103

Surface charge behavior and adsorption of surfactants on carbonate rocks

Rodriguez, Alfonso, M.S.

King Fahd University of Petroleum and Minerals (Saudi Arabia), 1992

U·M·I
300 N. Zeeb Rd.
Ann Arbor, MI 48106

SURFACE CHARGE BEHAVIOR AND ADSORPTION OF SURFACTANTS ON CARBONATE ROCKS

BY

ALFONSO RODRIGUEZ

A Thesis Presented to the

FACULTY OF THE COLLEGE OF GRADUATE STUDIES

KING FAHD UNIVERSITY OF PETROLEUM & MINERALS

DHAHRAN, SAUDI ARABIA

In Partial Fulfillment of the
Requirements for the Degree of

MASTER OF SCIENCE

In

PETROLEUM ENGINEERING

October 1992

KING FAHD UNIVERSITY OF PETROLEUM AND MINERALS
DHAHRAN, SAUDI ARABIA

COLLEGE OF GRADUATE STUDIES

This thesis, written by Mr. Alfonso Rodriguez under the direction of his Thesis Advisor and approved by his Thesis Committee, has been presented to and accepted by the Dean of the College of Graduate Studies, in partial fulfillment of the requirements for the degree of MASTER OF SCIENCE in Petroleum Engineering.

Thesis Committee:

H. Y. Al-Yousef
Dr. Hasan Al-Yousef
Thesis Advisor

Pierre Lichaa
Dr. Pierre Lichaa
Member

Dr. Hasan Al-Hashim
Member

Dr. Khalid Al-Fossail
Department Chairman

Dr. Ala H. Al-Rabeh
Dean, College of Graduate Studies

Date: 24-10-92

كلية الدراسات العليا
COLLEGE OF GRADUATE STUDIES

Dedicated to my

FAMILY

ACKNOWLEDGMENT

Acknowledgment is due to King Fahd University of Petroleum and Minerals for providing financial support during the period of my studies.

My sincere gratitude goes to Dr. Hasan Al-Yousef, Dr. Hasan Al-Hashim, and Dr. Pierre M. Lichaa who provided guidance throughout the course of this work.

Appreciation is also extended to Dr. Abdulaziz Al-Kaabi and the staff of the Petroleum Engineering Section, Division I of KFUPM Research Institute, for providing the facility and support for this research.

Thanks go to my friends and fellow students and to the staff and faculty at the Petroleum Engineering Deparment at King Fahd University of Petroleum and Minerals.

Last but not least, gratitude goes to Mario Salazar and the group of "Latinos" living in the area for their continuous encouragement and help during my stay in the Kingdom of Saudi Arabia.

TABLE OF CONTENTS

LIST OF TABLES

LIST OF FIGURES

ملخص الرساله

اسم الطالب : ردريجوز الفنصو

عنوان الدراسة : سلوك الشحنه الكهربائية للسطوح وامتصاص المواد الخافضة للتوتر السطحي على الصخور الجيريه .

حقل التخصص الرئيسي : هندسة البترول

تاريخ الشهادة : اكتوبر ١٩٩٢م

لقد تم دراسة تأثير المواد الخافضه للتوتر السطحي على سلوك الشحنه السطحيه للصخور الجيريه . كذلك تم عمل دراسات ستاتيكيه وديناميكيه للامتصاص لعينه واحده من المواد الخافضه للتوتر السطحي ذات الشحنه السالبه وعينتين ذات شحنه متعادله على الصخور الجيريه .

ان تفاعل الماء المالح مع سطح الصخور وكذلك طبيعة التفاعل بين المواد الخافضه للتوتر السطحي والصخور الجيريه قد تم تحليلها ودراستها من خلال دراسات الجهد الناتج عن الشحنات الكهربائيه السطحيه . كذلك تم دراسة تأثيردرجة الحراره وتركيب الماء المالح على معدل الامتصاص الاستاتيكي .

ان مركب ترايتون إكس ١٠٢ الخافض للتوتر السطحي ذات الشحنه الكهربائيه المتعادله قد أظهر أقل مستوى للامتصاص واكثر مستوى للاخراج على درجة حرارة ١٠٧ درجة مئويه وباستعمال الماء الذي تم تحضيره لدرجة ملوحة تعادل ٥٧٠٠٠ جزء من المليون . ان ميكانيكية الامتصاص لمركب بي ١٠٨٣ على درجات حرارة وملوحة مختلفه يمكن مقارنتها بطريقة جيده نسبياً مع قياسات الشحنات الكهربائية السطحية .

الماجستير في العلوم
جامعة الملك فهد للبترول والمعادن
الظهران - المملكة العربية السعودية
اكتوبر ١٩٩٢م

THESIS ABSTRACT

Name of Student : *RODRIGUEZ, ALFONSO*

Title of Study : *SURFACE CHARGE BEHAVIOR AND ADSORPTION OF SURFACTANTS ON CARBONATE ROCKS*

Major Field : *PETROLEUM ENGINEERING*

Date of Degree : *October 1992*

The influence of surfactants on the surface charge behavior of carbonate rocks was investigated. Static and dynamic adsorption studies were conducted for one anionic and two nonionic surfactants onto carbonate rocks.

The interaction of brine with the rock surface and the nature of the interaction between the surfactant and the carbonate rock were analyzed through zeta potential studies. The effects of temperature and brine composition on static adsorption density were also studied.

The nonionic surfactant Triton X-102 presented the lowest adsorption level and the highest desorption level at a temperature of 107 °C and a salinity of 57000 ppm synthetic brine. The adsorption of B1083 at different salinities and temperatures can be compared relatively well to the measurements of zeta potential.

MASTER OF SCIENCE

KING FAHD UNIVERSITY OF PETROLEUM AND MINERALS
Dhahran, Saudi Arabia

October 1992

CHAPTER 1

CHAPTER 1

INTRODUCTION

The word surfactant is a shortened form of the term "surface active agent" and denotes the outstanding property of these compounds. They tend to concentrate at the surface and interfaces of an aqueous solution and alter the surface properties [1].

Surfactant flooding is one of the enhanced oil recovery (EOR) techniques that can be successfully used for recovering light to medium oils from certain reservoirs following primary and secondary recovery techniques. However, one of the major factors affecting the success of surfactant flooding is the adsorption of surfactants onto reservoir rocks. In other words, surfactant flooding processes encounter problems due to loss of the surfactant by adsorption at the solid/liquid interface. In order to make a surfactant-based flood as effective as possible, careful evaluation and control of adsorption levels in the system of interest are essential [2].

Adsorption of surfactants on minerals is the result of a number of contributing forces, such as covalent bonding, coulombic interaction, ion exchange, desolvation of the polar group of the surfactant, hydrogen bonding, and hydrophobic and Van der Waals interactions [3].

The process of adsorption of surfactants on minerals such as calcite and

dolomite is not well understood because of the complexity of the interfacial region that exists when these minerals are immersed in an aqueous media [4].

The purpose of this research was to study the effect of surfactants on the surface charge behavior of carbonate rocks and to conduct static and dynamic surfactant adsorption tests. For this study two nonionic and one anionic surfactants were used.

CHAPTER 2

CHAPTER 2

LITERATURE REVIEW

Since 1915 the study of colloidal phenomena has been largely an experimental science. The oil industry has several applications which are based at least partially on colloidal phenomena.

The surface electrical properties of calcium carbonate, particularly those of calcite, dispersed in aqueous solutions have been studied using different electrokinetic and flotation techniques. Although these studies have provided some insight into the electrical state at this interface, they have also yielded many inconsistent and apparently contradictory results. For example, widely different zeta-potential values and diverse values of isoelectric points have been reported between pH 4 and 11 for these rocks [5].

Somasundaran and Agar [6] investigated the zero point of charge of calcite by measuring the streaming potential, solution equilibrium, and flotation response as a function of solution pH. The isoelectric point was shown to lie within the range of pH 8 to 9.5 which is in agreement with a recent study by Lichaa et al.[7].

Goujon and Mutaftschiev [8] determined the heat of immersion of calcite in water and found it to be very high because of a partial surface descomposition of about 30% during thermal treatment.

Smith [9] investigated the electrokinetic properties for oxide/aqueous solution interfaces and found that the isoelectric point of a solid-solution interface can lead to a value for the inner layer capacity.

Smallwood [10] used the technique of microelectrophoresis and measured the zeta potential of calcite and aragonite in the presence of calcium and magnesium. It was shown that both ions were adsorbed to the mineral's surfaces and caused an increase in the positive charge.

Smith and Shonnard [11] investigated the role of modifying agents in flotation using zeta potential measurements and concluded that barite is more positively charged than calcite.

Leaist [12] studied the behavior of porous calcium hydroxide that is exposed to aqueous hydrochloric acid and concluded that coupled ionic diffusion in solutions-saturated pore can produce subsurface dissolution or precipitation without chemical reaction.

Sharma et al.[13] investigated the surface charge and zeta potential of Ottawa sand, baked, and unbaked Berea sandstone using three different techniques: streaming potential, electrophoresis, and potentiometric titrations. It was concluded that streaming potential and electrophoresis are the most appropriate methods for determining surface potential.

Menezes and Sharma [14] measured the zeta potential of the solid-liquid and liquid-liquid interfaces for pure surfactants and mud components. It was concluded that the cationic surfactant CTAB caused a decrease in the zeta potential of the silica-water interface, and at concentrations below the CMC, the zeta potential becomes positive. The same study concluded that the anionic surfactant, SDS, caused a negative increase in the zeta potential.

Mannhardt et al. [2] investigated the surface charge of Berea sandstone, Indiana limestone and Baker dolomite in concentrated electrolyte solutions. In their study, it was concluded that limestone and dolomite were dramatically influenced by the pH and the presence of multivalent ions. Similar results were obtained by Lichaa et al.[7] on carbonate rocks.

Andersen and Sumasundaran [15] used electrophoresis for determining the mechanism of amine, sulfate, and oleate adsorption on calcite and concluded that both oleate and sulfate adsorb due to chemical interaction, while amines adsorb mainly due to electrostatic interactions. It was shown that the dependecy of the zeta potential on the solid-to-liquid ratio can be used to delineate the mechanism of adsorption of surfactants on certain minerals.

Trushenki et al.[16] found the existence of maximum adsorption near the critical micellar concentration (CMC) range followed by a minimum for a system of Berea sandstone, Mahogany petroleum sulfonate system and

isopropylalcohol micellar fluid at 43 °C.

Bae and Petrick [17] concluded that there is a maximum adsorption of sulfonates in Berea core systems. Novosad [18] also found a maximum value in his study for Berea cores. Celik et al.[19] confirmed the existence of a maximum value of adsorption by taking into account the precipitation and dissolution of surfactant.

Hanna and Somasundaran [20] found that adsorption depends on the kind of surfactant and inorganic dissolved species that are present in the system.

Trogus et al.[21,22] performed static and dynamic adsorption experiments on Berea sandstone using nonionic and anionic surfactants having different alkyl chain length. They reported an increase in the level of adsorption with increasing chain-length of anionic surfactants and the opposite for nonionic surfactants. Lawson [23] also observed that multivalent cations increase the adsorption of anionic surfactants.

Glover et al.[24] observed severe retention of surfactants in a system containing considerable amount of divalent ions, most probably due to the precipitation of surfactants.

Smith et al.[25,26] and Lawson [27] showed that residual oil has no effect

on adsorption, while Malmberg and Smith [28] found that a smaller slug of surfactant injected, and oil decrease the adsorption.

Glinsmann [29] conducted dynamic adsorption experiments on water-wet Berea sandstone at residual oil saturation. A surfactant and alcohol were injected at various NaCl concentrations. He concluded that sulfonate losses were minimum for systems in the middle phase region where the oil recovery was maximum. Boneau et al.[30] demostrated that oil-wet cores adsorb more sulfonate than water-wet cores.

Hanna and Sumasundaran [31] used limestone samples and compared the adsorption properties of two distinct limestones in terms of mineralogical composition. Agricultural limestone presented a lower adsorption density than Bedford limestone. Figdore [32] compared the effect of NaCl and $CaCl_2$ on the adsorption of anionic ethoxylate surfactants. He concluded that calcium-surfactant complex has a significant role in the adsorption process and must be accounted for whenever divalent metal cations are present.

Shakeel [33] investigated the adsorption of surfactans on Saudi Arabian limestones. He carried out static adsorption experiments of petroleum sulfonate, ethoxylated sulfonates, and nonionic surfactants. He concluded that the increase in ionic strength generally resulted in higher sulfonate adsorption at high sulfonate concentrations. He also found that above the isoelectric point (pH = 8.3) the adsorption of sulfonates was marginal.

Al-Hashim et al. [34] concluded that the degree of surfactant adsorption was generally found to change by altering the brine concentration.

Poirier and Cases [35] investigated the adsorption of anionic surfactants onto silicate minerals by comparing the adsorption of sulfonate onto quartz and kaolinite surfaces. In both cases, the anionic surfactants molecules adsorbed onto the negatively charged surface.

Xu et al.[36] carried out a study of adsorption of anionic-nonionic and cationic-nonionic surfactant mixtures on kaolinite. It was found that the anionic surfactant adsorption was enhanced by the presence of the nonionic surfactant and vice-versa in the pre-CMC region.

Little research, especially in brines containing significant amounts of electrolytes, has been conducted on reservoir rock surface charge measurements. However, a major contribution has been reported recently on Saudi Arabian carbonate rocks [37].

The objective of this reseach was to study the effect of surfactants on surface charge behavior of carbonate rocks and to determine what kind of surfactant has less adsorption capacity on carbonate rocks.

CHAPTER 3

CHAPTER 3

EXPERIMENTAL EQUIPMENT AND PROCEDURES

Zeta potential measurements and static and dynamic adsorption experiments were conducted. The description of the equipment, materials, and experimental procedures are presented in this chapter.

3.1 EXPERIMENTAL EQUIPMENT

3.1.1 Zeta potential equipment

Zeta potential measurements were made using an equipment composed of a Zeta-meter 3.0 unit and a microscope module. It includes a precision DC power supply, a microprocessor for zeta potential calculation, a control for the microscope illuminators and a keypad for tracking colloids. The power supply provides regulated-stable DC power between 0 and 300 volts.

The colloidal suspension to be tested is first placed in an electrophoresis cell where colloid particles are conveniently viewed and tracked with the microscope module.

3.1.2 Static adsorption equipment

The following equipment was used to perform the static adsorption tests:

ASAP 2000 was used in the determination of the surface area of the

carbonate rock. A multi-wrist shaker was used to simulate hand shaking, and a clinical centrifuge was used to precipitate solids.

3.1.3 Dynamic adsorption equipment

A schematic diagram of the core flooding setup is shown in Figure 3.1. The major components of the apparatus are: A rubber sleeve to load the two composite cores, a hassler type stainless steel core holder, a constant rate pump to inject fluids and apply overburden pressure, a convection oven to control the temperature, and graduated tubes.

3.2 MATERIALS

Carbonate rocks from Saudi Arabian reservoirs in Uthmaniyah area were used in this study.

3.2.1 Preparation of cores

Core plugs of 1 inch in diameter and 1.5 inch in length were drilled from a two inch-diameter full core samples. The core samples were cleaned with toluene for 2 weeks.

A helium porosimeter and a liquid permeameter were used to determine the porosity and permeability of the core plugs. Basic core properties, such as dimension of the samples, porosity and permeability are shown in Table 3.1.

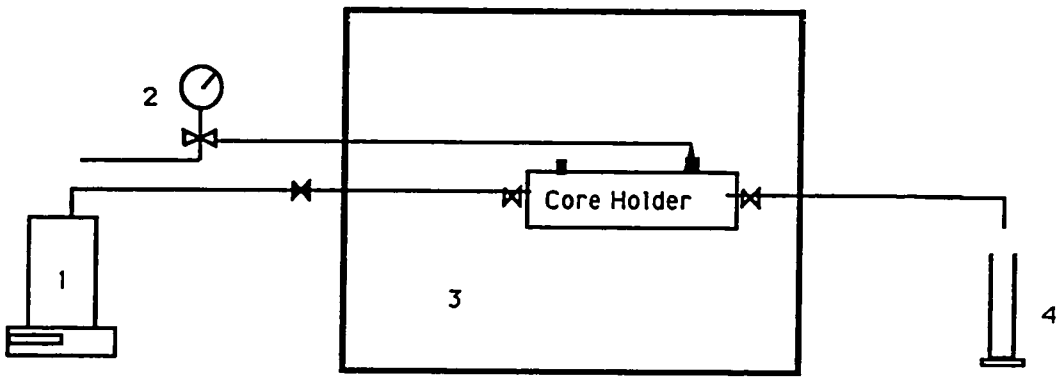

1. Pump
2. Overburden pressure gauge
3. Oven
4. Fluid collector tube

Figure 3.1 Schematic diagram of the core flooding setup.

Table 3.1 Physical Properties of carbonate Core Samples Used in the Adsorption Study

SAMPLE	LENGTH (cm)	POROSITY (fraction)	PERMEABILITY (md)	SURFACTANT
A	4.6	0.205	76	B1083
B	4.7	0.210	97	
C	3.75	0.195	363	X-102
D	5.0	0.200	510	
E	4.7	0.196	1488	Sapogenat T-100
F	4.4	0.190	1588	

The core samples were reused after cleaning with methanol for 8 hours followed by steam for 16 hours.

3.2.2 Surfactants

Figure 3.2 shows the chemical constitution of anionic and nonionic surfactants used in this study. B1083 is an ethoxylated anionic surfactant with an activity of 21 %. Sapogenat T-100 is a tributylphenol polyglycol ether nonionic surfactant with an activity of 100%, and Triton X-102 is a polyethoxylated octyl phenol nonionic surfactant with an activity of 100%.

3.2.3 Brines

A synthetic brine with a salinity of 25000 ppm TDS simulating the brine in which the cores were preserved, was used for the zeta potential experiments to study the surface charge of the carbonate rock. This ionic strength is also the upper limit of the Zeta-Meter system. Table 3.2 shows the geochemical analysis for this brine.

Table 3.3 shows the geochemical analysis for the synthetic brine used for the dynamic and static adsorption experiments. The concentration of 57000 ppm TDS and the composition shown in the table simulate the injection water used in the field.

NONIONIC SURFACTANTS

-Sapogenat T-100

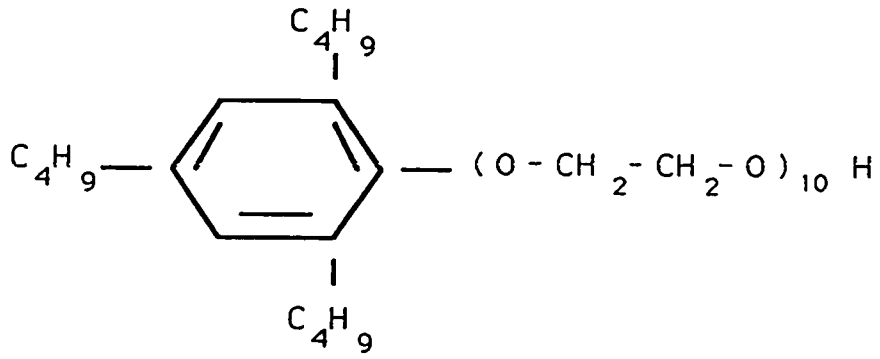

-Triton X-102

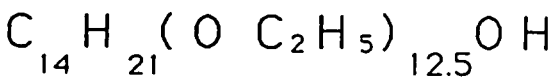

ANIONIC SURFACTANT

-B1083

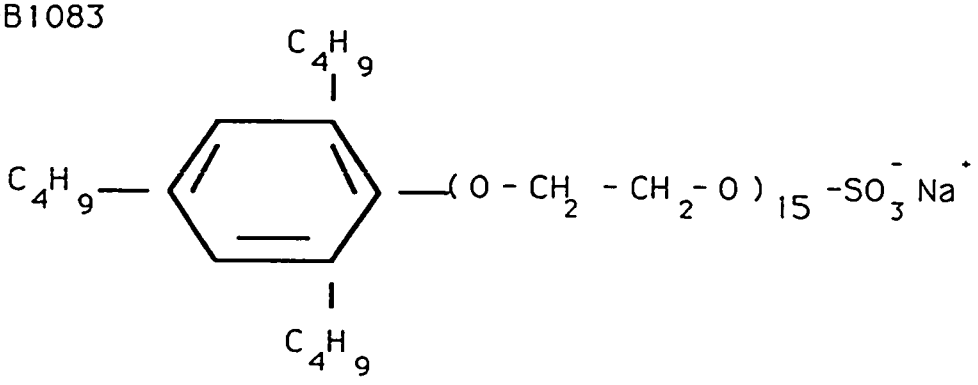

Figure 3.2. Chemical constitution of the surfactants used (43).

Table 3.2 Geochemical Analysis of 25000 ppm Synthetic Brine

ANALYTE	CONCENTRATION (ppm)
Sodium	1220
Calcium	7910
Magnesium	36.9
Chloride	15636.1
Potassium	197
Total	25000

Table 3.3 Geochemical Analysis of 57000 ppm Synthetic Brine

ANALYTE	CONCENTRATION (ppm)
Sodium	18300
Calcium	650
Magnesium	1440
Sulfate	4290
Chloride	32200
Bicarbonate	120
Total	57000

3.3 EXPERIMENTAL PROCEDURES

3.3.1 Zeta potential measurement

The procedure used for measuring the zeta potential [14,37] consists of crushing the rock into colloid particles, followed by equilibration in aqueous solutions of different surfactants and 25000 ppm preserving brine for 12 hours. The sample was then dried in an oven for 30 minutes at 80 °*C*. The sample was suspended in deionized water or 25000 ppm TDS brine to perform the zeta potential measurements as a function of pH. The required pH of the solution was adjusted by adding either sodium hydroxide or hydrochloric acid. After allowing sufficient time for equilibrium, the sample was placed in an electrophoresis cell and observed under a microscope. A DC voltage was then applied, and the particle movement toward the electrodes was observed. The particle relative velocity, called "electrophoretic mobility", is proportional to the zeta potential which is measured by the system.

3.3.2 Static adsorption tests

Static surfactant adsorption tests were conducted at low and high temperatures. A sample of 2 grams of crushed rock was contacted with 10 ml of known surfactant concentration. The sample was conditioned for 6 hours at 25 or 90 °*C* in a shaking thermostated water bath. The sample was centrifuged at room temperature for 15 minutes at 3000 rpm and kept

overnight in a water bath at the same temperature without shaking in order to ensure that equilibrium has been attained. The supernatant was analyzed for residual surfactant concentration using a UV-260 spectrophotometer.

3.3.3 Dynamic adsorption tests

The carbonate cores were cut, cleaned with toluene for 2 weeks and dried in a vacuum oven at 110 °*C* for 24 hours. Then, the cores were saturated under vacuum with 57000 ppm synthetic brine. The core samples were mounted in the core holder and 800 psi of overburden pressure was applied. The test temperature was set at 107 °*C*. Several pore volumes of brine were injected into the core samples followed by injection of several pore volumes of surfactant solution at a constant flow rate. The surfactant solution was followed by displacement with 57000 ppm brine until surfactant concentration at the core outlet approached a zero value. The effluents were then collected and analyzed using a UV-260 spectrophotometer.

3.3.4 Analysis of effluents

A calibration curve for each surfactant used was established. The absorbance of different surfactant concentrations was entered into the autocalibration option of the spectrophotometer. Absorbance was established according to the following procedure: The reference cell was filled with 57000 ppm brine while the sample cell was filled with the effluent to be analyzed.

The detection wavelenght was set at 241.4 nm for B1083 and X-102 surfactants while for Sapogenat T-100 surfactant it was set at 500 nm. Each sample was mounted and the absorbance of UV light was measured. The absorbance obtained was compared to the calibration curve previously established and thus, the surfactant concentration was obtained. It is appropiate to point out that the calibration curves are not affected by brine composition. Therefore, they were used for analyzing the effluent and supernatants at different salnities.

3.3.5 Surface area measurement

The BET method [33] was used to determine the surface area of the carbonate rock using nitrogen gas. This method is based on the following equation :

$$P/\,V\,(P_o - P) \;=\; 1/\,V_m\,C_g \;+\; (C_g - 1)\,P\,/\,C_g V_m\,P_o \qquad (1)$$

where :

V = Volume of gas adsorbed at pressure P.

V_m = Volume of the gas monolayer.

P_o = Saturation pressure of adsorbate gas at the experimental temperature.

C_g= A constant related experimentally to the heats of adsorption and liquefaction of the gas.

A plot of $P/V(P_o\text{-}P)$ versus P/P_o gives a straight line if the adsorption follows the BET equation. The value V_m may be obtained from the slope and intercept of the line. Thus, the surface area can be determined from the interrelationship of the gas density, molecular weight of the gas and the effective area covered by each gas molecule.

The specific surface area obtained for the rock chips was 0.317 m^2/g. The surface area measurement for the crushed rock sample of Saudi Arabian limestone was 13.2 m^2/g as was previously reported [33].

The static adsorption density was calculated from the analysis of supernatants:

$$\Gamma_s = (C_i - C_r)\ (1/S.A)\ (1/1000) \quad (2)$$

where :

Γ_s = Static adsorption density, g/m^2.

C_i= Initial surfactant concentration, g/l.

C_r = Residual surfactant concentration, g/l.

S = Solid concentration, g/cc.

A = Surface area of crushed sample, m^2/g.

The dynamic adsorption density was calculated by taking into account the total amount of surfactant adsorbed at a specific surfactant concentration:

$$\Gamma_d = ((C_i - C_o) * V_i) * (1/ S_c A_c) (1/1000) \quad (3)$$

where :

Γ_d = Dynamic adsorption density, g/m^2

C_i = Initial surfactant concentration, g/l

C_o = Average outlet surfactant concentration, g/l

V_i = Volume injected, cc

S_c = Core sample weight, g

A_c = Surface area of rock chips, m^2/g.

CHAPTER 4

CHAPTER 4

RESULTS AND DISCUSSION

This chapter presents the results and discussion of the zeta potential, and the static and dynamic adsorption studies carried out with two nonionic and one anionic surfactants onto carbonate rocks.

4.1 ZETA POTENTIAL MEASUREMENTS

The generation of surface charge when a solid is in contact with aqueous solution is common to almost all systems. One of the major factors influencing the adsorption process is the electrical interactions within the environment of an electrical double layer which consists of a compact surface charge layer and a diffuse layer of counterions. Since in reservoir rocks, a double layer exists between the rock's minerals and the pore-filling brine, an understanding of the charge generation and the structure of the double layer is important when the surfactant solution at different concentrations makes contact with the carbonate rock.

Figure 4.1 shows a schematic of the double layer. Closest to the carbonate rock surface is a layer of hydrated counterions, called the stern layer. Some counterions remain on the surface, while others diffuse away decreasing in concentration toward the brine , forming the Gouy diffuse layer in which cation and anion concentration gradually approaches that in the free brine.

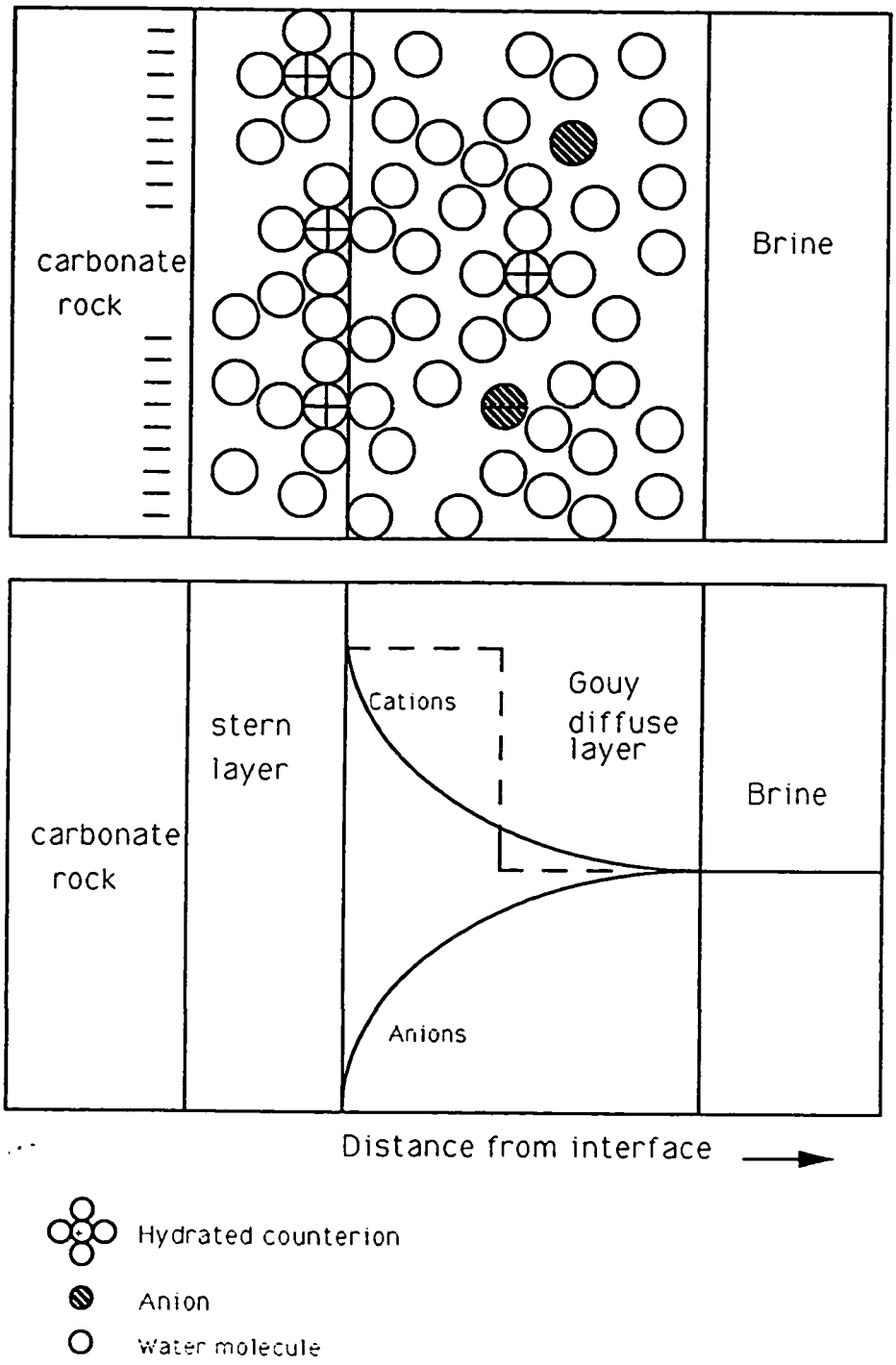

Figure 4.1 Schematic of the double layer (38)

The Stern layer thickness depends primarily on the size of the hydrated counterion, which varies slightly with brine concentration. The Gouy layer varies dramatically in thickness with brine concentration; it is thickest for fresh brines and virtually zero in concentrated brines [38].

Zeta potential measurements were obtained for the surfactants considered in this study. The surfactant concentrations were varied from 0.25 % to 4.0 %.

4.1.1 Effect of pH

Figure 4.2 and Tables A.1 and A.2 show the effect of pH on zeta potential for the carbonate rock used. It can be concluded that the surface charge is pH dependent and can be either positive or negative.

The explanation for this behavior is that when the carbonate rock is dissolved in water, chemical species will be produced such as : H_2CO_3, HCO_3^-, CO_3^-, Ca^{++}, $CaOH^+$,and $Ca(OH)_{2(s)}$.

When calcite, the main component of the carbonate rock tested, reaches equilibrium with the water at a certain pH value, an excess of the negative HCO_3^- and CO_3^- will exist. On the other hand, low pH values will favor an excess of Ca^{++}, $CaHCO_3^+$, and $CaOH^+$ [6].

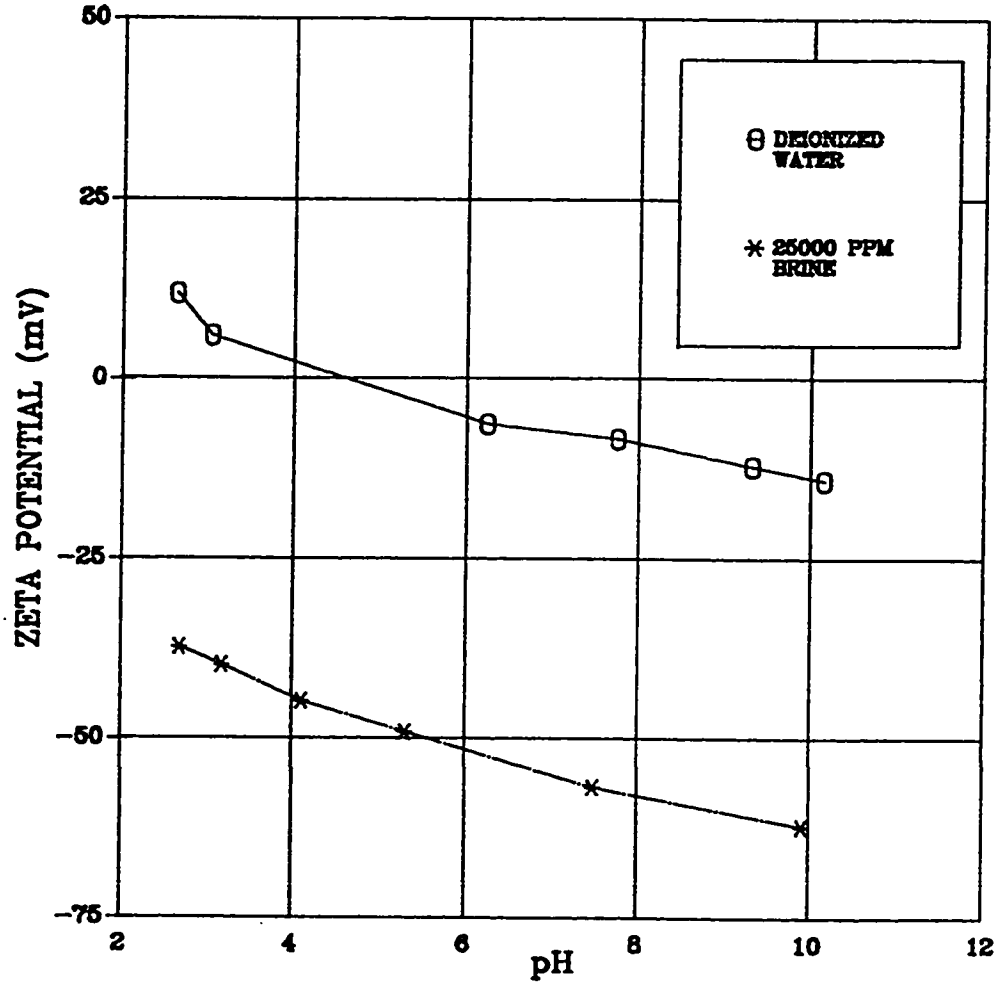

Figure 4.2 Variation of zeta potential of a carbonate rock with pH tested in deionized water and 25000 ppm preserving brine.

4.1.2 Isoelectrical point

The pH value at which the surface is electrically neutral, is known as the "isoelectrical point" (I.E.P). The zero point of charge is a characteristic property of the solid. Electrokinetic measurements yield the pH at which the particle has a zero charge,i.e., the zeta potential is zero.

For the carbonate rock studied, the isoelectrical point was found to be equal to 4.2 in deionized water. Some investigators have found calcite to have I.E.P greater than 8.0 [6,34] while others have found it to be completely negative over the complete range of pH. Isoelectrical points between pH 4 and 11 have been reported by many investigators [2,4,5,6,34]. The variation in the results obtained by different investigators can be attributed to the complex dissolution behavior of calcite and its sensitivity to sample pretreatment and equilibration, and to the ionic strength and composition of the aqueous medium.

4.1.3 Effect of salinity

Figure 4.2 illustrates that an increase in salinity produced an increase in the negativity of the zeta potential of the carbonate rock. It is also important to point out that the zeta potential of the carbonate rock is negative over the whole range of pH values when tested in the synthetic brine. Therefore, anionic and nonionic surfactants are most suitable since they will have less

adsorption than a cationic surfactant.

4.1.4 Effect of concentration and type of surfactant

Figures 4.3 through 4.8 and Tables A.3 - A.32 illustrate the effect of surfactant type and concentration on the zeta potential. Variation of the zeta potential of the carbonate rock with pH for different concentrations and type of surfactant tested in deionized water is shown in Figures 4.3 - 4.5. It can be observed that the isoelectrical point of the carbonate rock is decreased by the increase in the concentration of the anionic surfactant (Figure 4.5). The nonionic surfactants presented a small change which can be attributed to the fact that most of the nonionic surfactants are a mixture of anionic and cationic surfactants. Therefore, the net effect of the nonionic surfactants was to decrease the surface charge of the carbonate rock toward zero. It is to be noted that the Sapogenat T-100 and B1083 presented a larger variation of zeta potential than Triton X-102 when the surfactant concentration was increased.

Figures 4.6 through 4.8 show the variation of the zeta potential of the carbonate rock with pH for different concentrations and type of surfactant tested in 25000 ppm brine. In general, the effect of the nonionic surfactants was small and the trend was similar to the one obtained in deionized water.

The increase in concentration of the anionic surfactant made the zeta potential more negative. This can be explained by the fact that the anionic

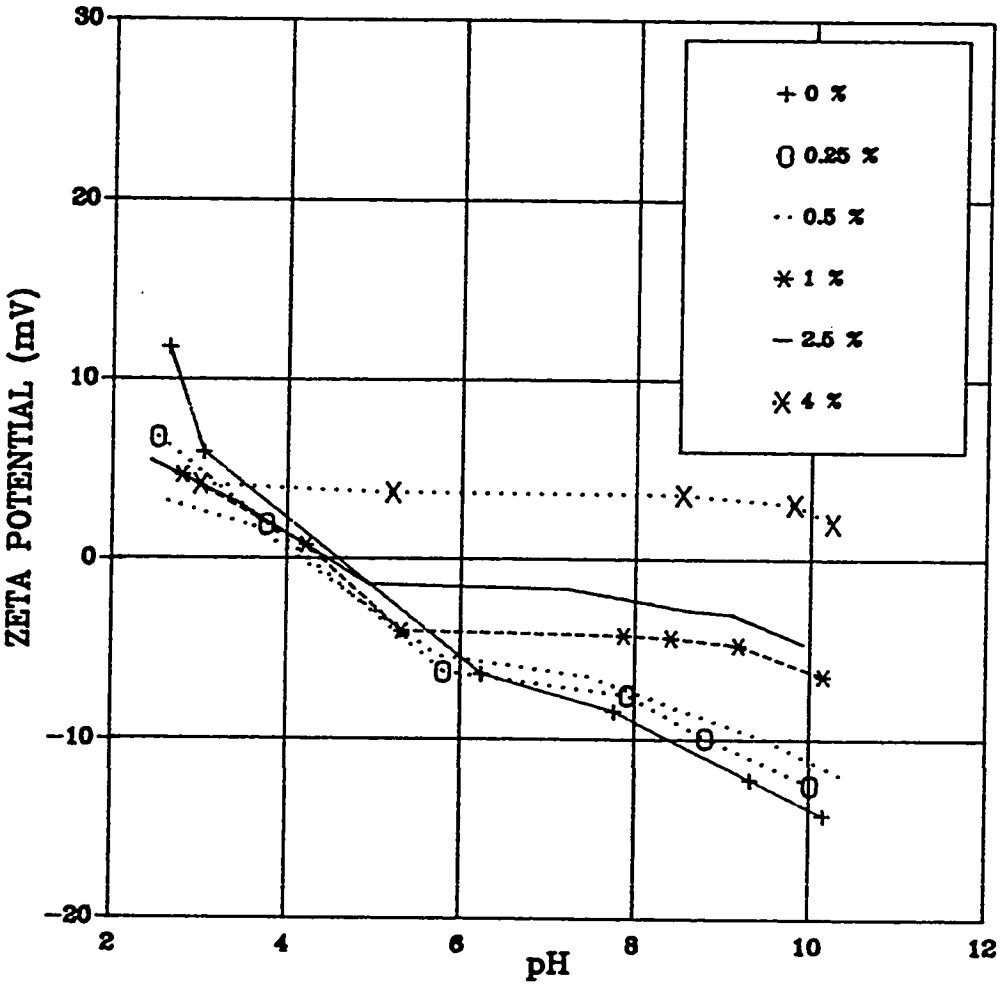

Figure 4.3 Variation of zeta potential of a carbonate rock with pH for different concentrations of Sapogenat T–100 surfactant tested in deionized water.

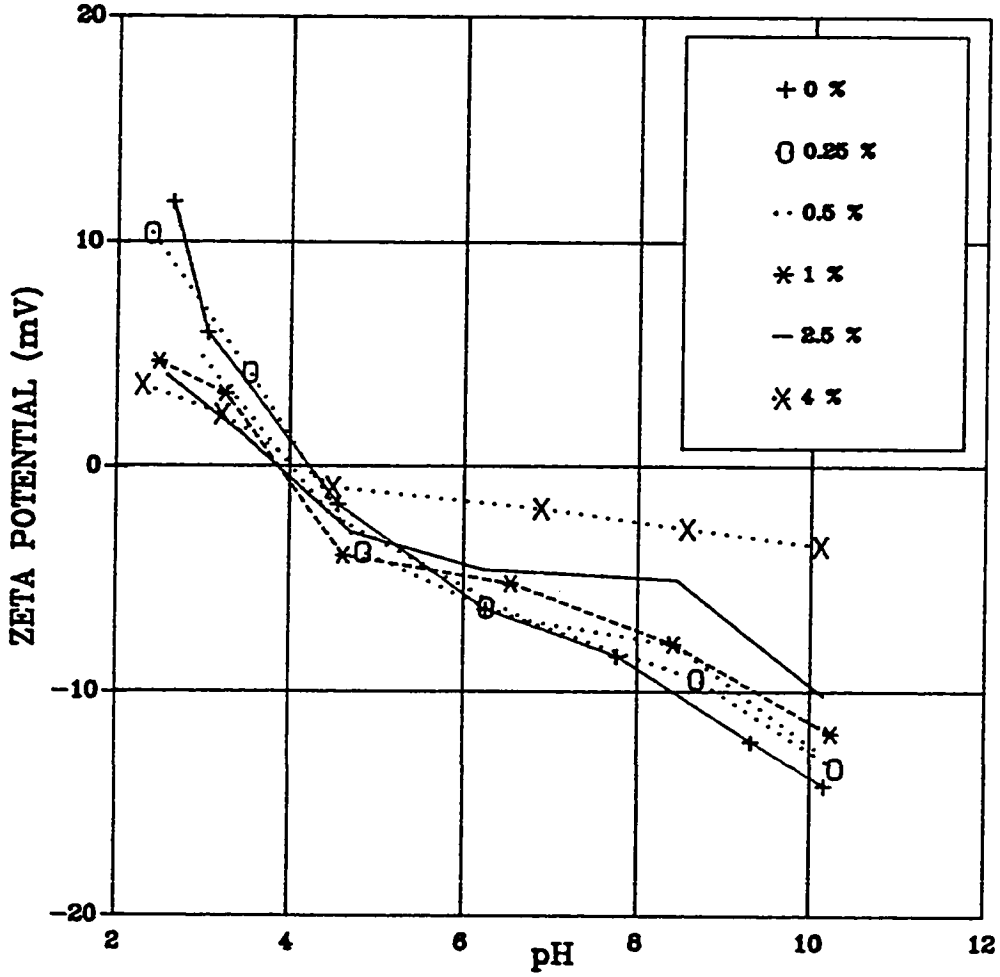

Figure 4.4 Variation of zeta potential of a carbonate rock with pH for different concentrations of X-102 surfactant tested in deionized water.

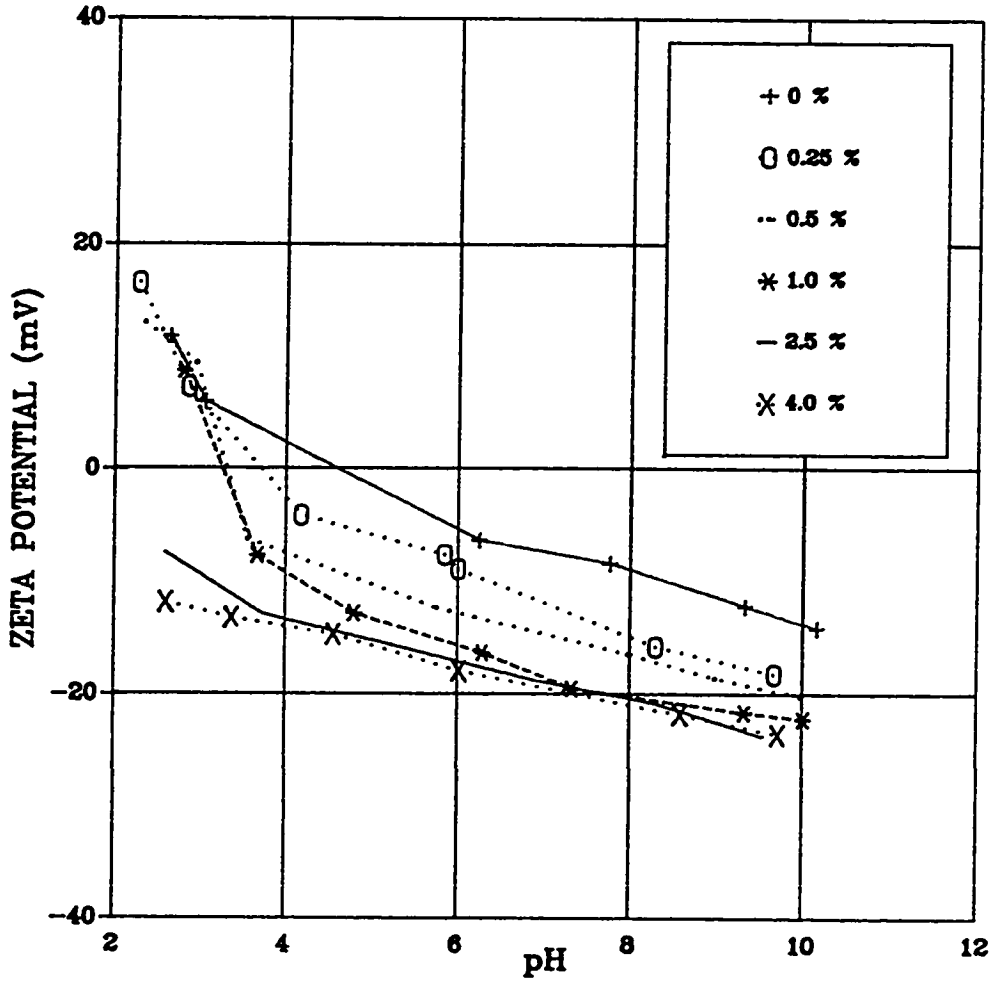

Figure 4.5 Variation of zeta potential of a carbonate rock with pH for different concentrations of B1083 surfactant tested in deionized water.

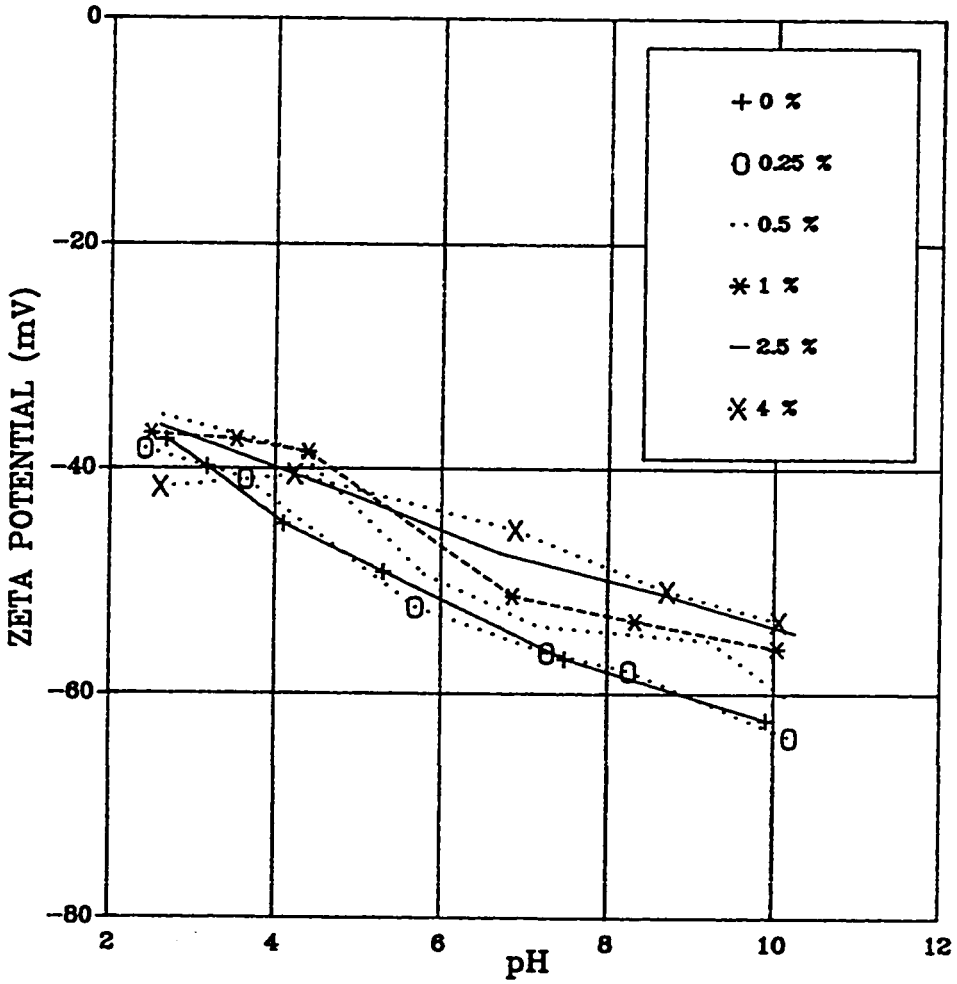

Figure 4.6 Variation of zeta potential of a carbonate rock with pH for different concentrations of Sapogenat T-100 surfactant tested in 25000 ppm preserving brine.

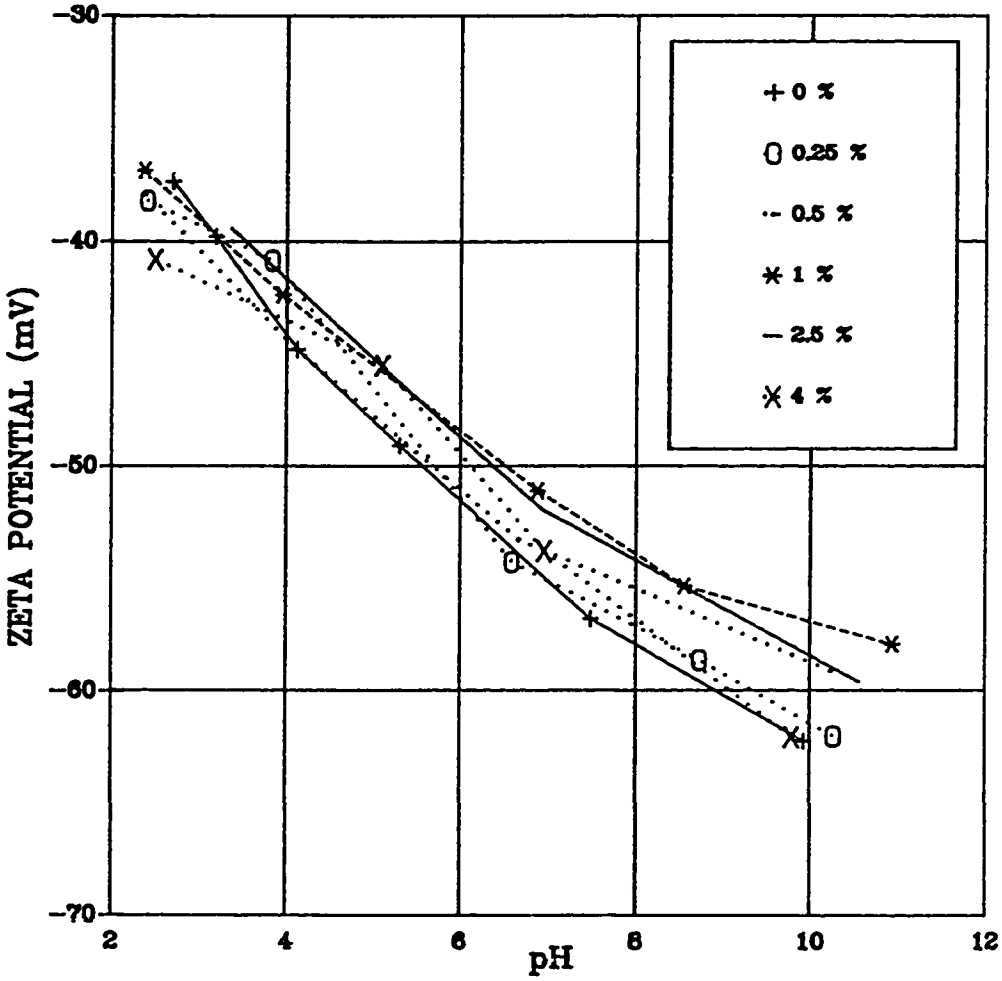

Figure 4.7 Variation of zeta potential of a carbonate rock with pH for different concentrations of X-102 surfactant tested in 25000 ppm preserving brine.

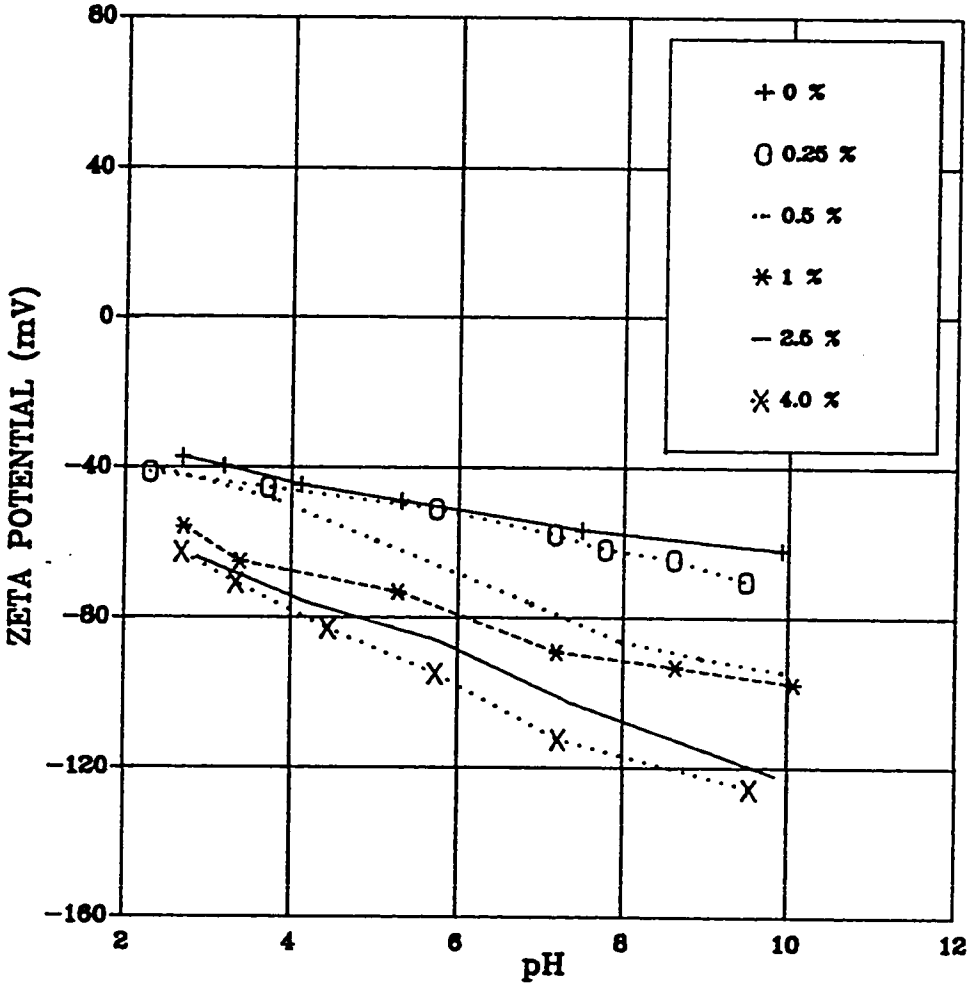

Figure 4.8 **Variation of zeta potential of a carbonate rock with pH for different concentrations of B1083 surfactant tested in 25000 ppm preserving brine.**

surfactant has a certain nonelectrostatic affinity for the surface of the carbonate rock and hence tends to enrich the interface, but may not be considered part of the surface since the surfactant and the surface of the carbonate rock exhibit the same sign.

A comparison of zeta potential for Sapogenat T-100, Triton X-102, and B1083 at a pH of 8.0 is presented in Figures 4.9 and 4.10. All the surfactants tested presented a natural pH close to 8.0. Thus, the comparison was restricted to this value which is close to the pH of reservoir environments.

Figure 4.9 illustrates the variation of zeta potential of the carbonate rock with surfactant concentration for anionic and nonionic surfactants tested in deionized water at a pH of 8.0. The zeta potential of the nonionic surfactants is seen to decrease toward zero with increase in surfactant concentration. The zeta potential of the anionic surfactant decreases continuously with an increase in surfactant concentration up to 1 %, then it remains constant above this concentration.

Figure 4.10 shows the variation of zeta potential of the carbonate rock with surfactant concentration for anionic and nonionic surfactants tested in 25000 ppm at a pH of 8.0. The zeta potential of the nonionic surfactants is seen to remain relatively constant. The zeta potential of the anionic surfactant changes sharply with an increase in surfactant concentration up to 0.5%, then it changes at a constant rate with increasing surfactant concentration.

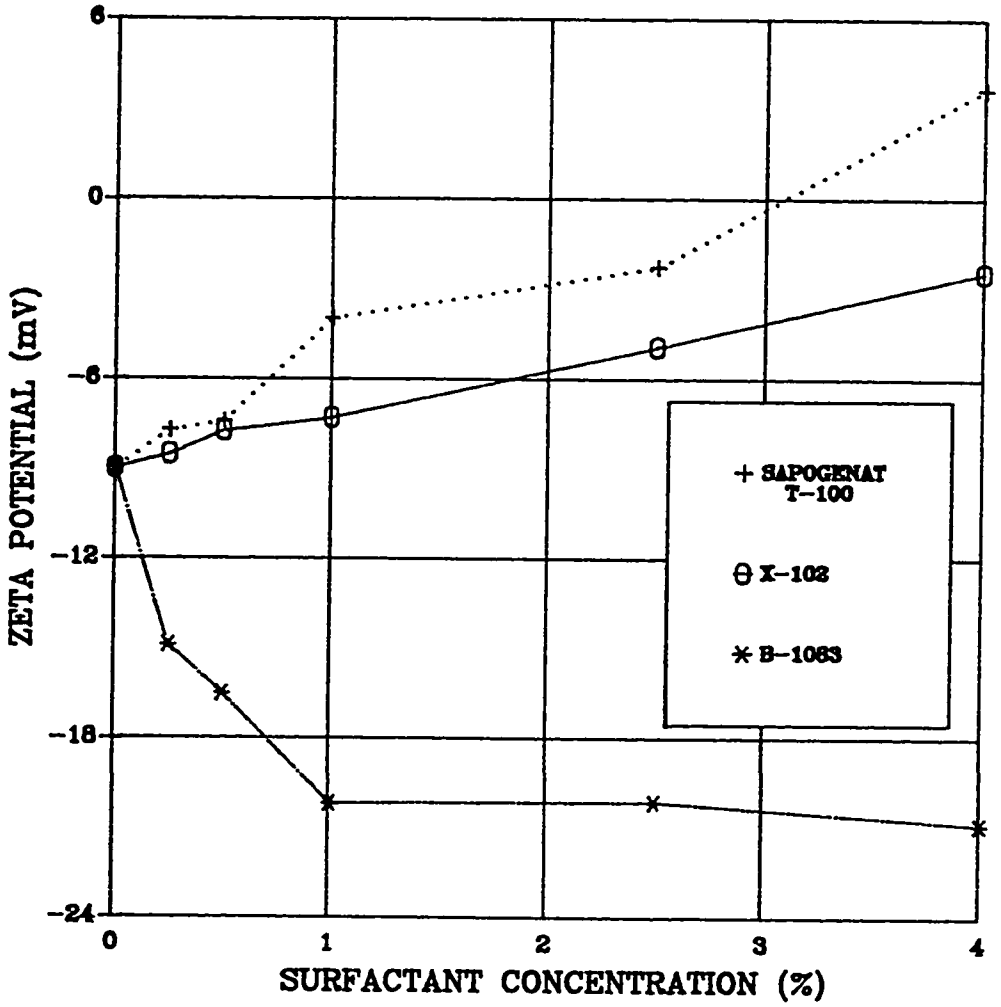

Figure 4.9 Variation of zeta potential of a carbonate rock with concentration for different surfactants tested in deionized water and at a pH of 8.0

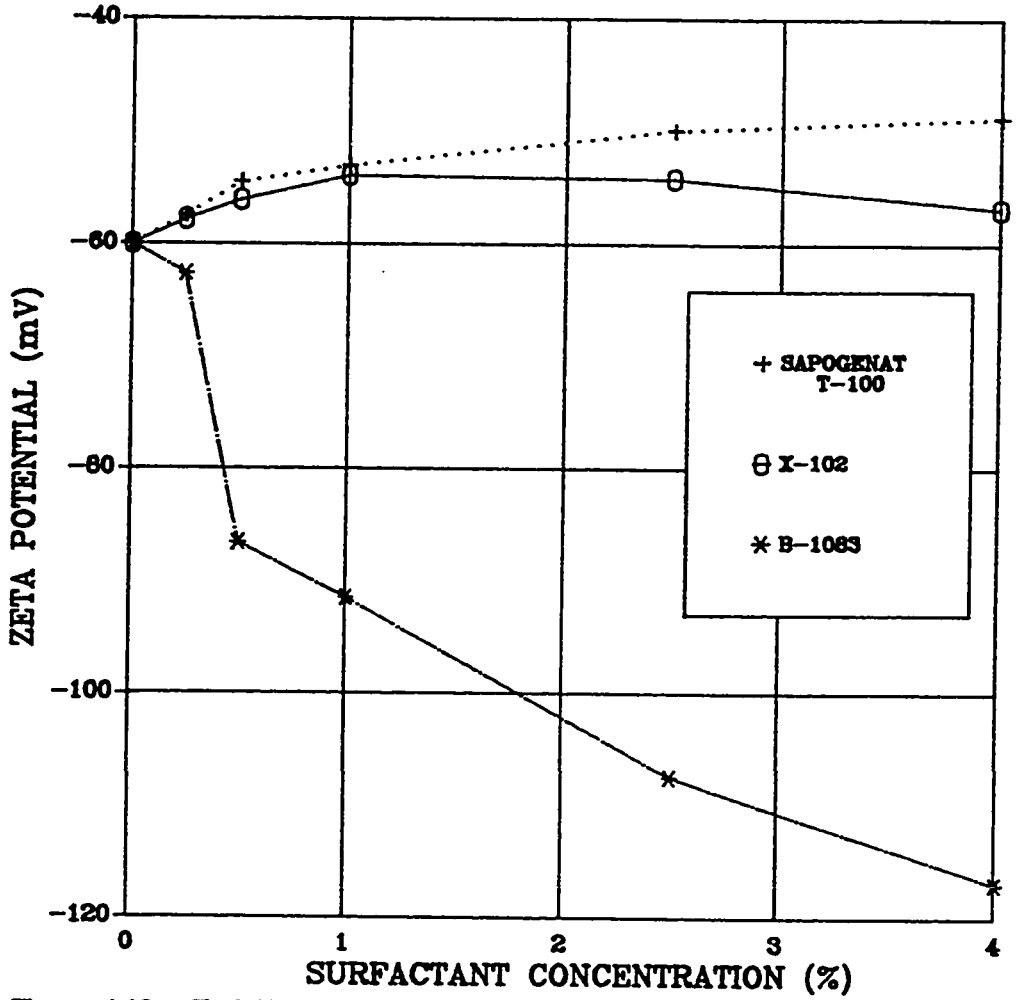

Figure 4.10 Variation of zeta potential of a carbonate rock with concentration for different type of surfactants tested in 25000 ppm preserving brine and at a pH of 8.0.

4.2 STATIC ADSORPTION RESULTS

4.2.1 Calibration curves

The experimental evaluation of the adsorption of surface active agents from solution at the solid-liquid interface usually involves the measurement of the change in concentration of the active solute in the solution that results from adsorption. Thus, a UV-260 spectrophotometer was used to analyze the supernatant of the static adsorption tests and the effuents of the dynamic adsorption tests. Figures 4.11-4.13 and Tables B.1-B.3 show the calibration curves for the nonionic and anionic surfactants used in this study. Multiple linear regression was used in order to fit the calibration data for the Triton X-102 and the B1083.

4.2.2 Static adsorption isotherms

The usual method for evaluating the adsorption mechanism is through the adsorption isotherm. Giles et al. [40] have produced a general classification of isotherms with various shapes that were subsequently justified theorically [41].

Figure 4.14 and Table B.4 show the adsorption isotherms on crushed carbonate rocks with different types of surfactants at 90 °C. These data reasonably indicate a Langmuir-type isotherm. Sapogenat T-100 is the surfactant that had the highest adsorption. Thus, it was decided to carry out

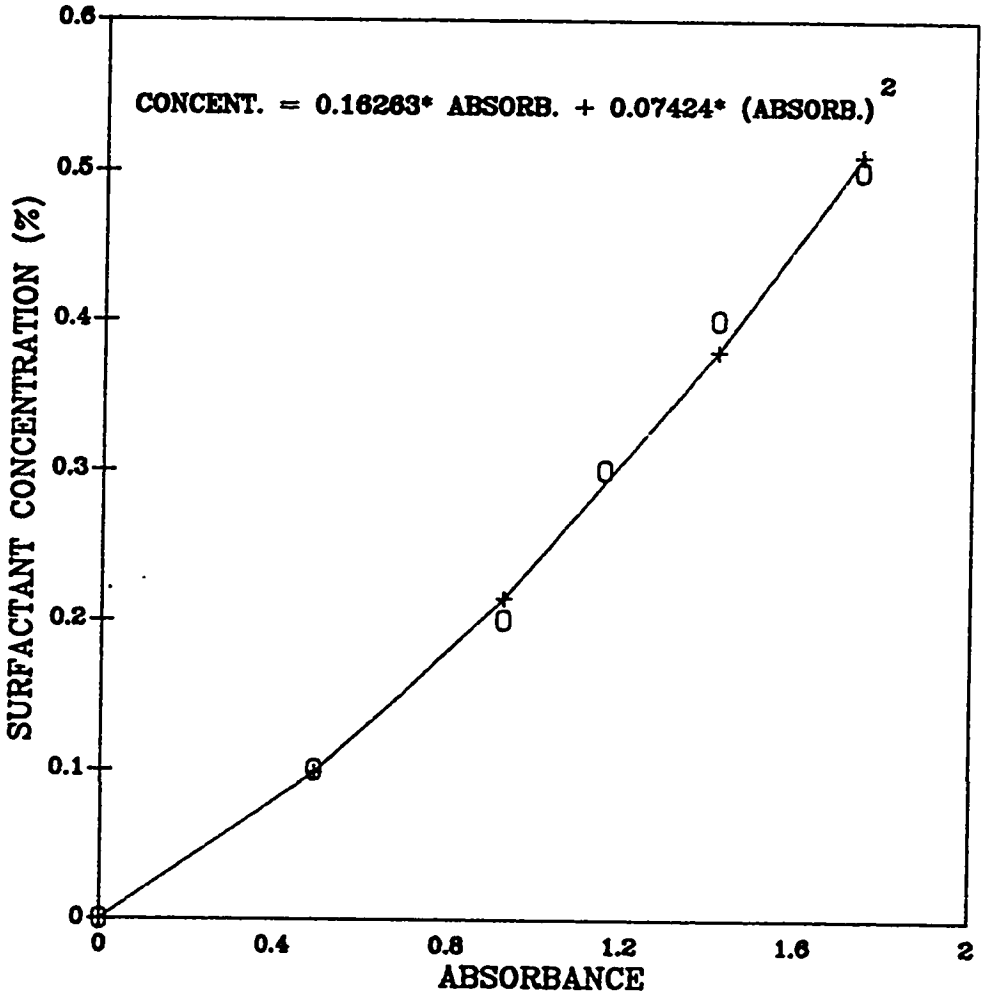

Figure 4.11 Calibration curve for Sapogenat T-100 at a wavelenght of 500 nm.

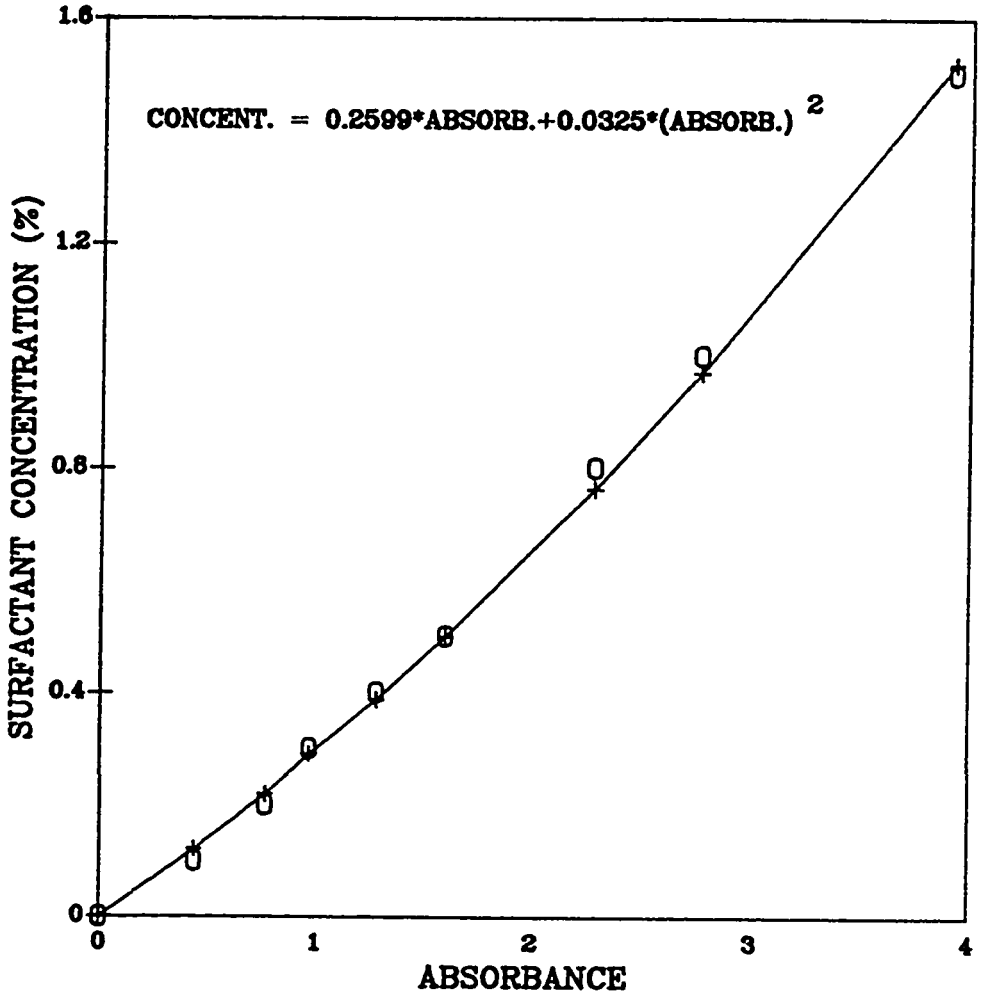

Figure 4.12 Calibration curve for x-102 at a wavelenght of 241.4 nm.

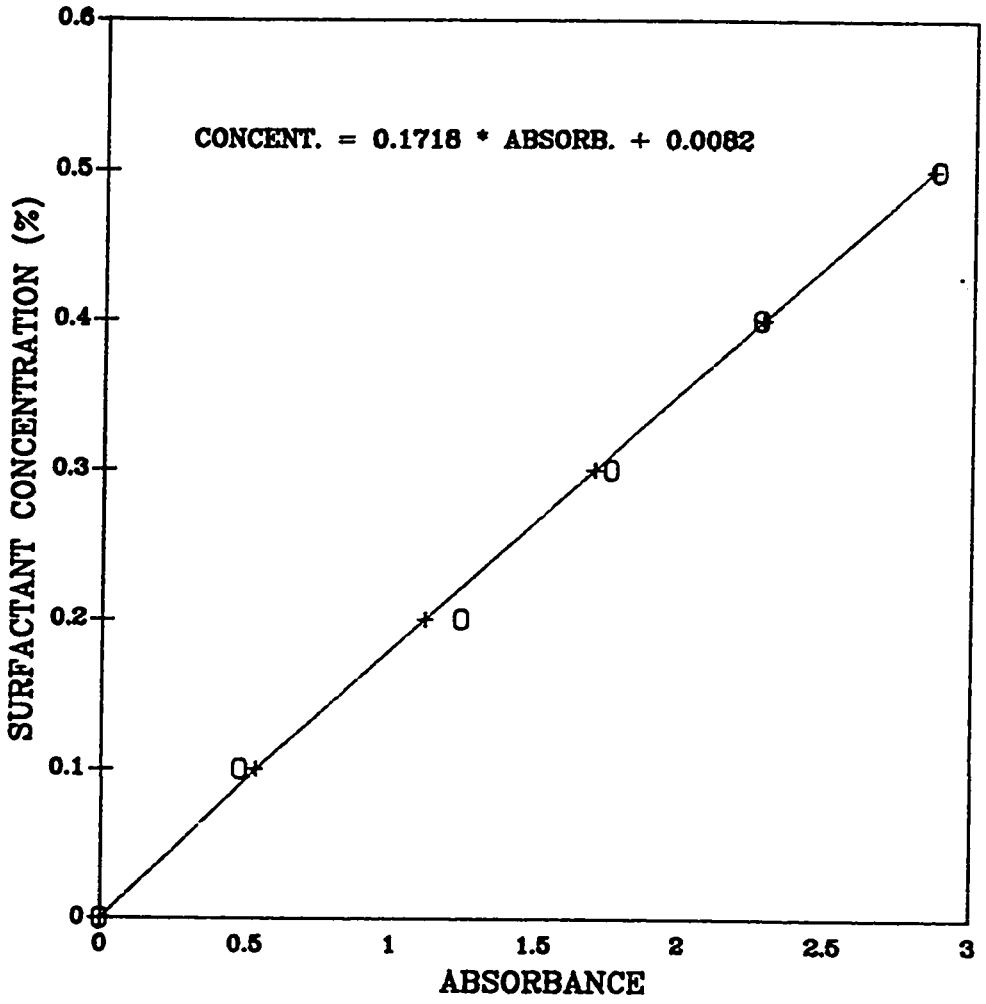

Figure 4.13 Calibration curve for B1083 at a wavelenght of 241.4 nm.

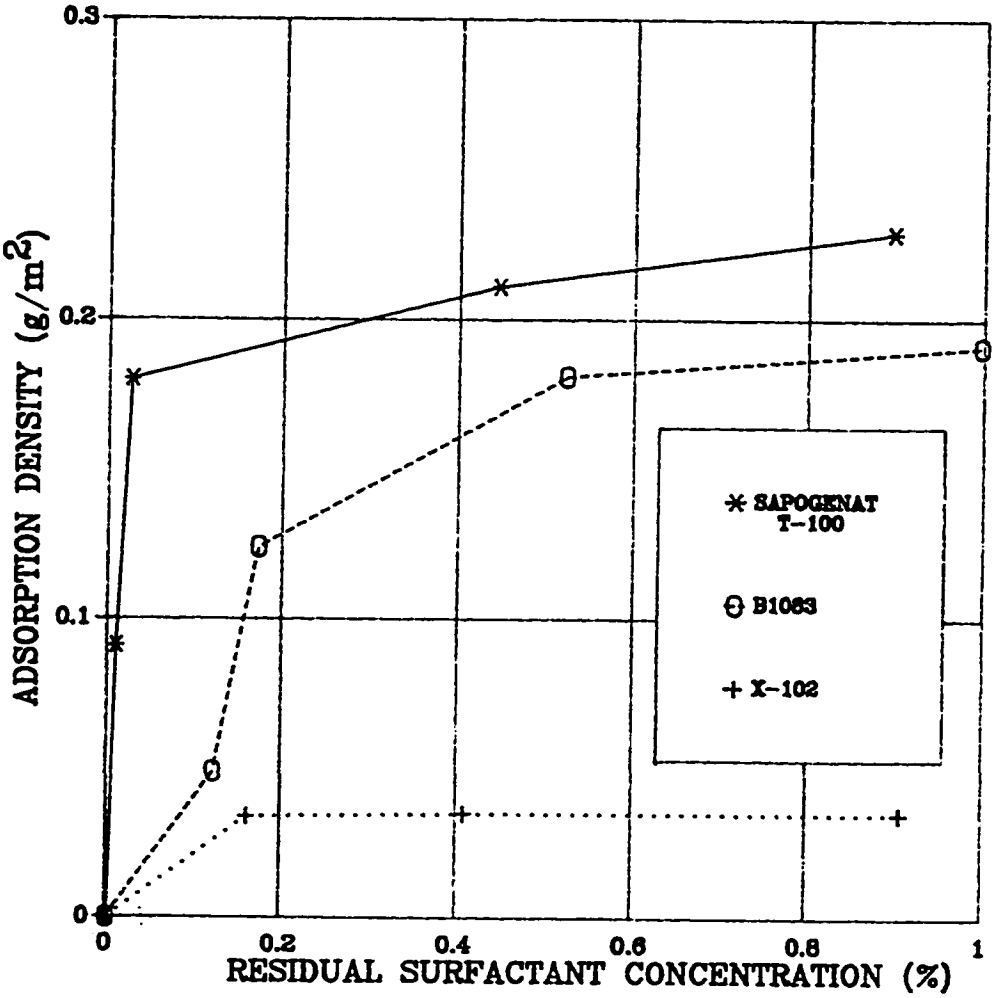

Figure 4.14 Variation of static adsorption density of a carbonate rock with concentration for different types of surfactants at 57000 ppm and 90 °C.

static adsorption experiments with Triton X-102 and B-1083 at room temperature using 25000 ppm and 57000 ppm brines in order to study the effect of temperature and salinity on adsorption. The results are given in Figures 4.15 and 4.16 and Tables B.4 - B.6 respectively. It can be seen that the adsorption isotherm of the Triton X-102 is altered with an increase in salinity. In spite of the fact that the salinity and composition of brine is altered, it is to be noted that the general shape of adsorption isotherms for B1083 remained the same.

The trend of adsorption increase with salt concentration is consistent with data published by others [20,23,32]. The effect of temperature can be seen also in Figures 4.15 and 4.16. Adsorption of B1083 and X-102 increased markedly with temperature. However, the shape of the adsorption isotherms is relatively maintained.

4.3 DYNAMIC ADSORPTION RESULTS

4.3.1 Effluent profiles

Figures 4.17-4.19 and Tables B.7-B.15 present the effluent profiles of adsorption and desorption. The outlet concentration of B1083 and Sapogenat T-100 did not reach the injected concentration even after injecting ten pore volumes of surfactant solution. The effluent concentration profile of Triton X-102 steadily increased to reach the injected level at about ten pore volumes

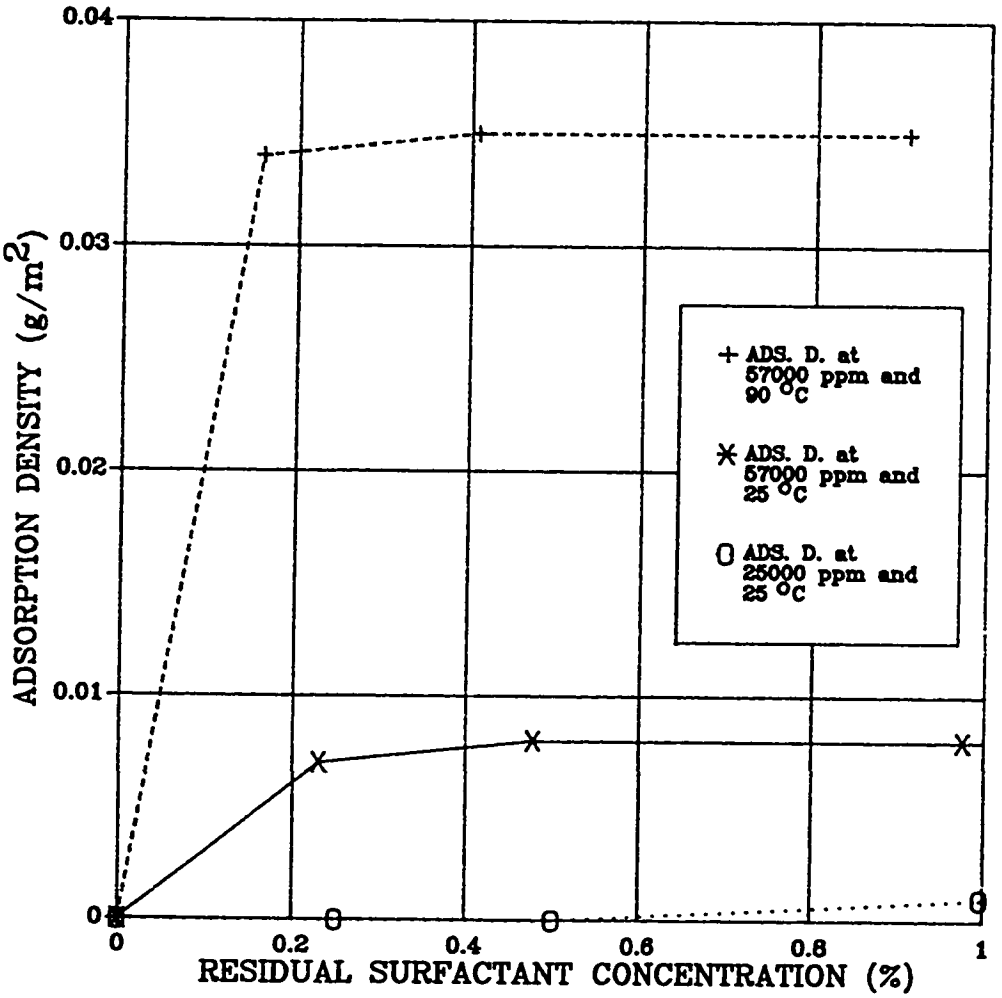

Figure 4.15 Variation of static adsorption density of a carbonate rock with concentration for Triton X-102 at different temperatures and salinities.

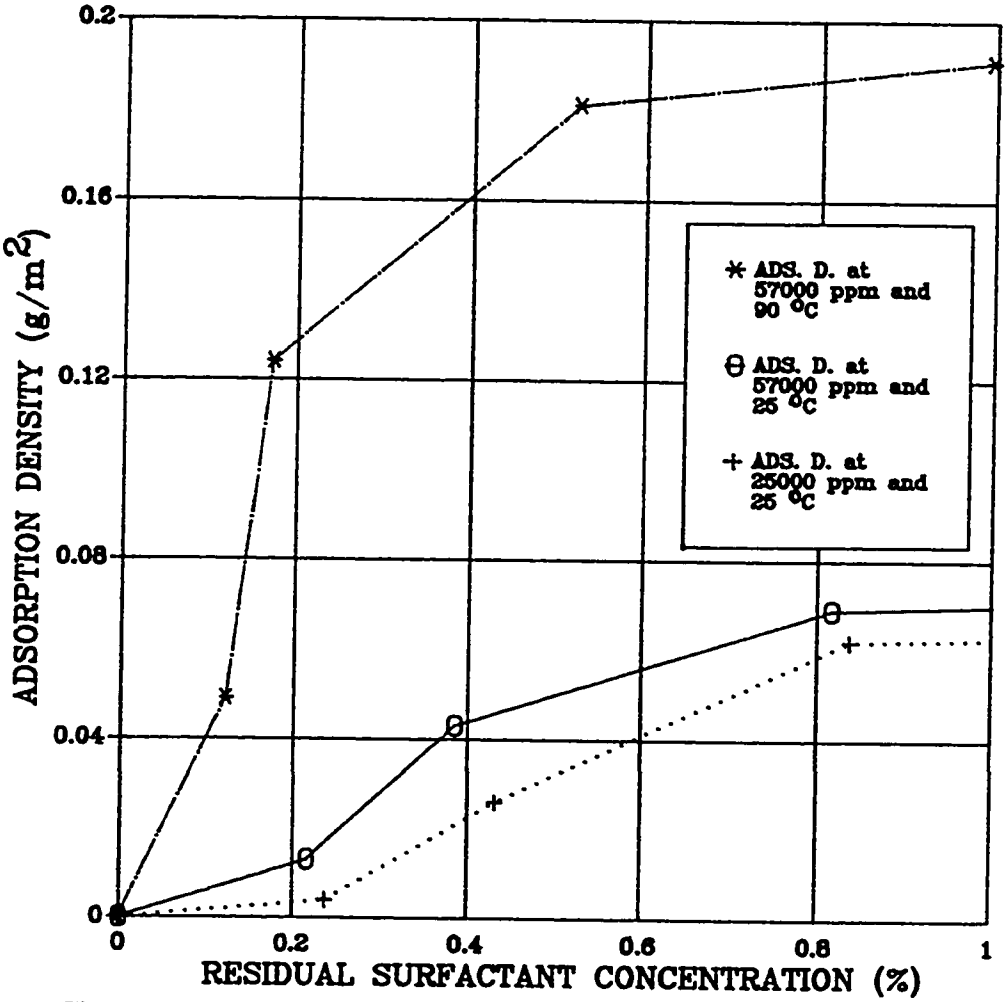

Figure 4.16 Variation of static adsorption density of a carbonate rock with concentration for B1083 at different temperatures and salinities.

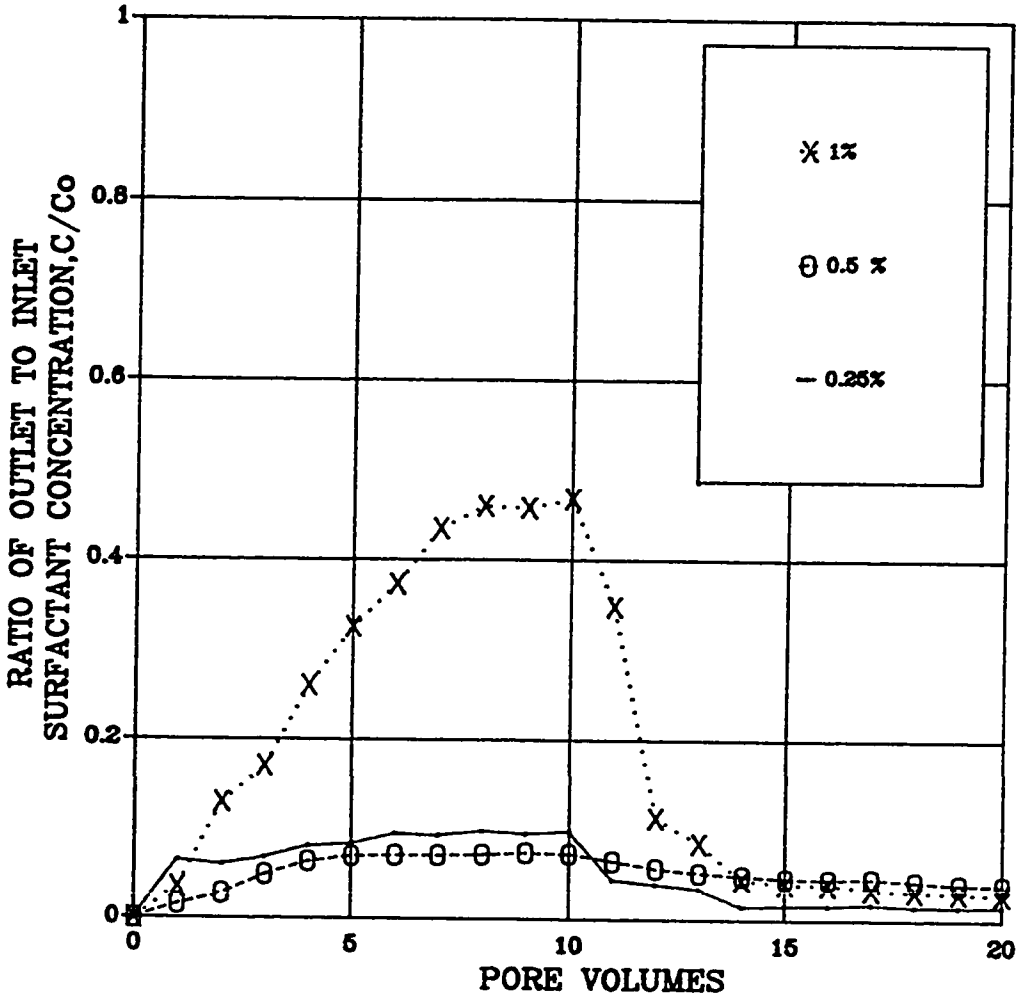

Figure 4.17 Adsorption and desorption profiles of Sapogenat T–100 at 2 cc/min, 57000 ppm, and 107 °C.

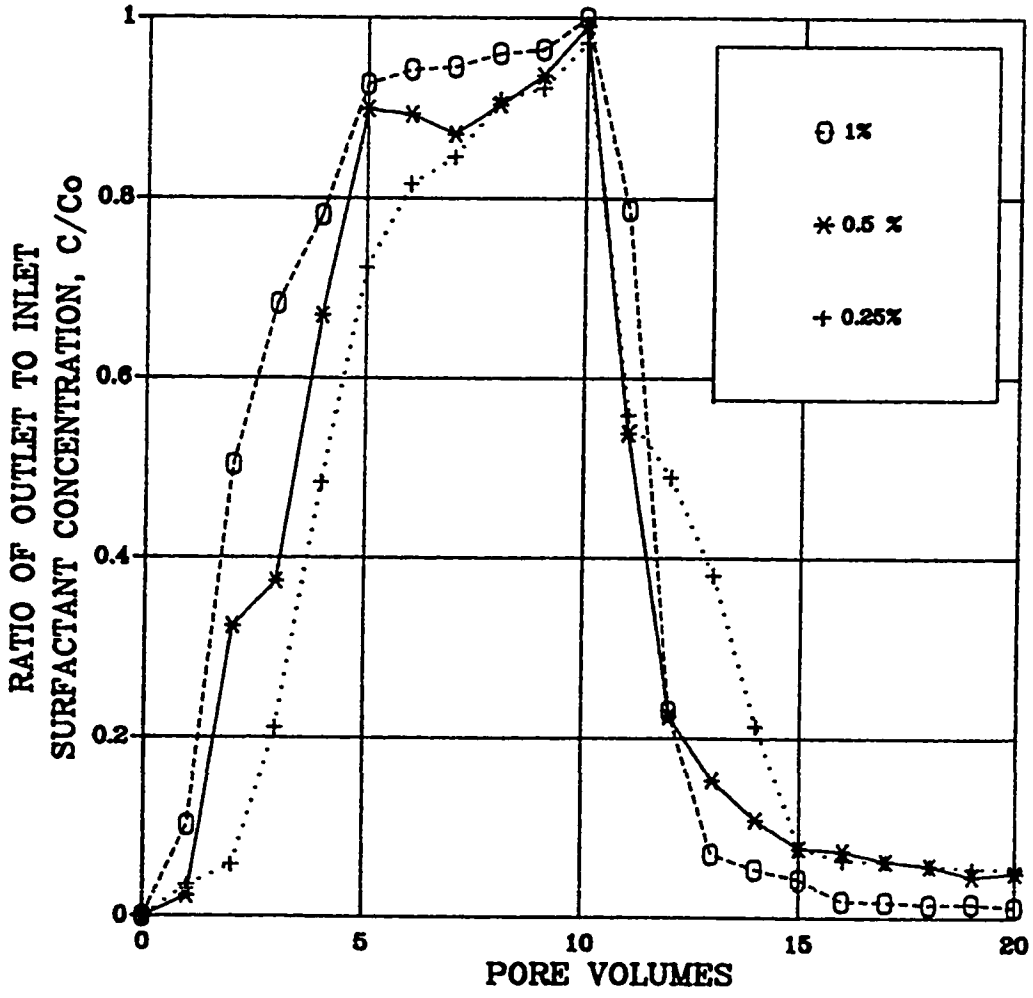

Figure 4.18 Adsorption and desorption profiles of Triton X-102 at 2 cc/min., 57000 ppm, and 107 °C.

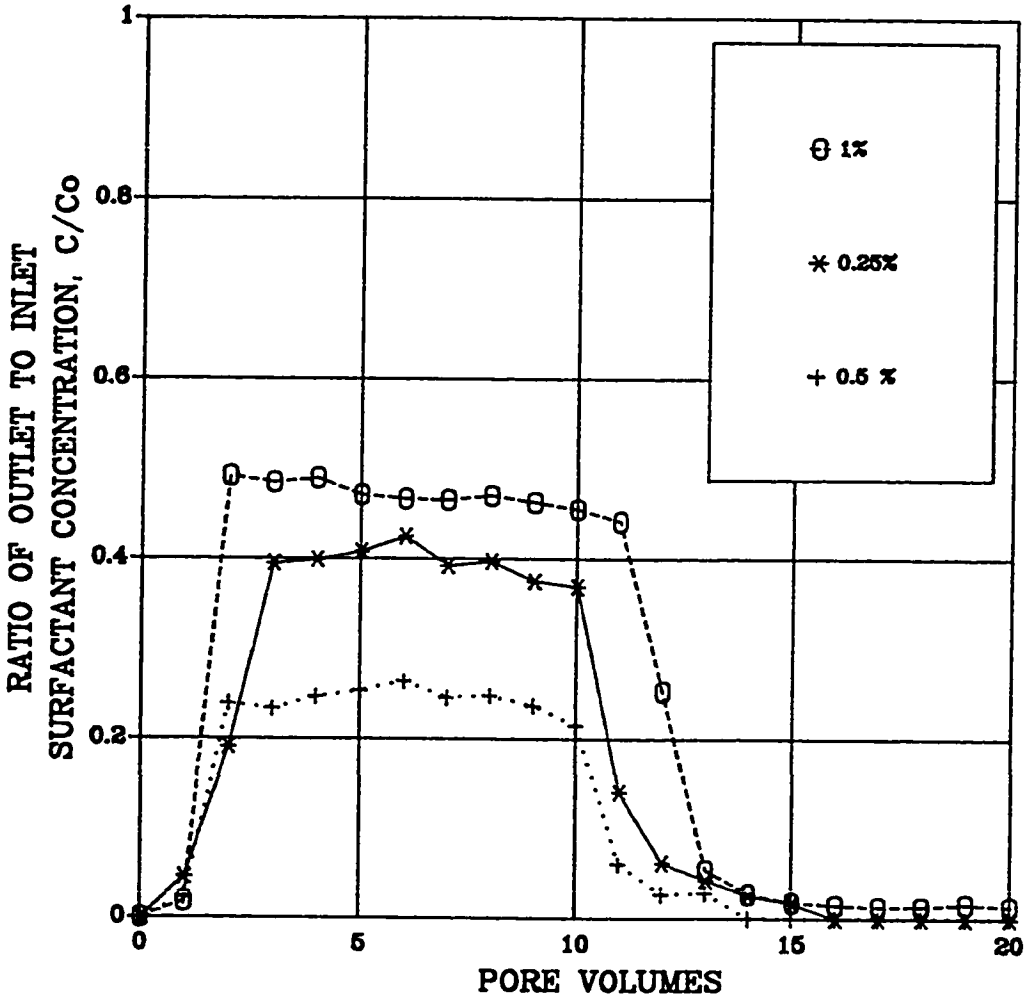

Figure 4.19 Adsorption and desorption profiles of B1083 at 2 cc/min, 57000 ppm, and 107 °C.

To determine if adsorption was limited by the amount of surfactant injected, another series of floods were conducted with B1083 at a lower flow rate of 0.5 cc/min until the surfactant at the outlet was equal to the inlet concentration. Figures 4.20 - 4.22 and Tables B.13 - B.18 show that the decrease in the flow rate resulted in a higher adsorption and also that the injected concentration was reached after injecting more than 20 pore volumes. Thus, the equilibrium time for adsorption is flow rate dependent. Bae and Petrick [17] found that at concentrations below 1%, adsorption is dependent on flow rate. In this study the time required for adsorption equilibrium was found to decrease with increasing the concentration, contrary to the findings of Bae and Petrick [17]

The adsorption profiles obtained in this study are in agreement with Trogus et al. [22] who obtained similar shapes of the breakthrough curves that were obtained in the present study. They used nonionic and anionic surfactants, and Berea cores where it was necessary to inject with some surfactants more than 80 pore volumes to obtain the injected concentration at the outlet.

Novosad [39] studied the retention of pure sulfonate, petroleum sulfonate, and synthetic sulfonate on Berea cores and concluded that the average concentration can be obtained by averaging the inlet and the maximum outlet concentrations. The results reported in the present study show the existence of

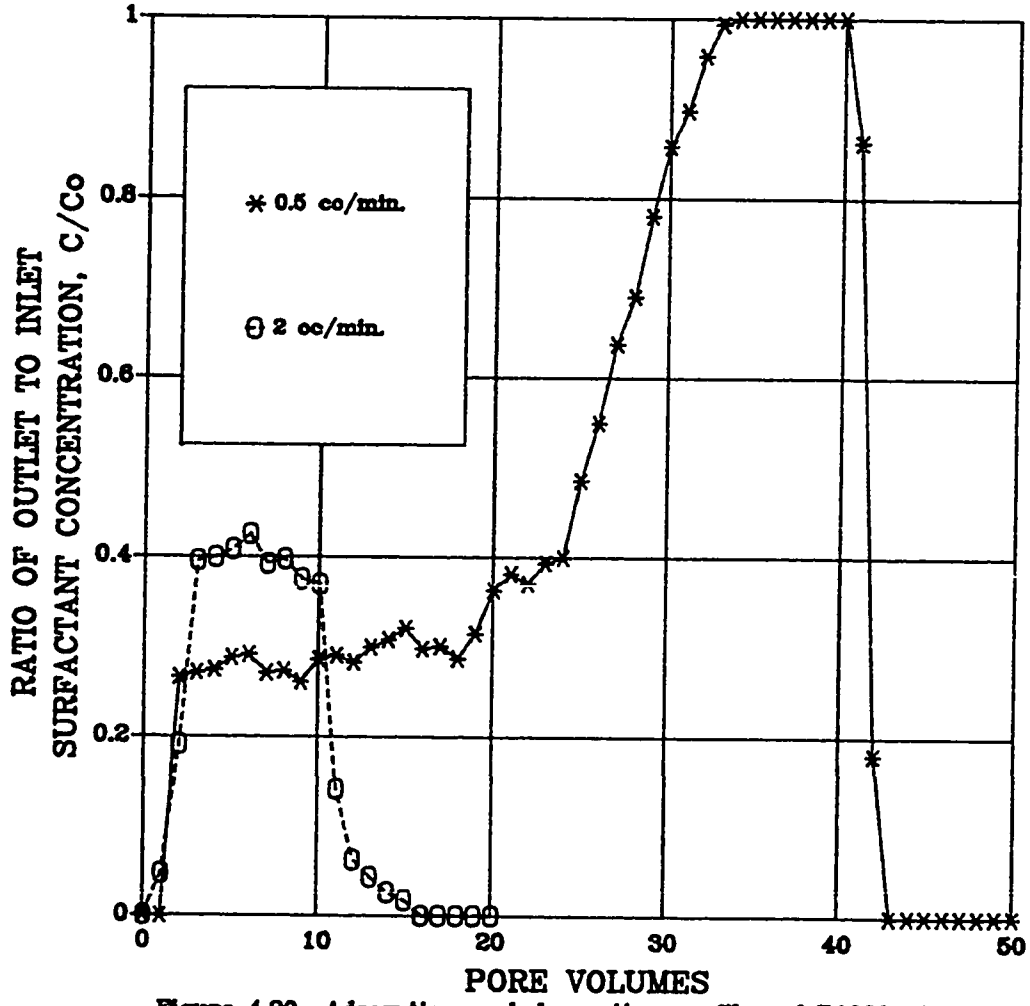

Figure 4.20 Adsorption and desorption profiles of B1083 at a concentration of 0.25%, 57000 ppm, 107 °C, and different flow rates.

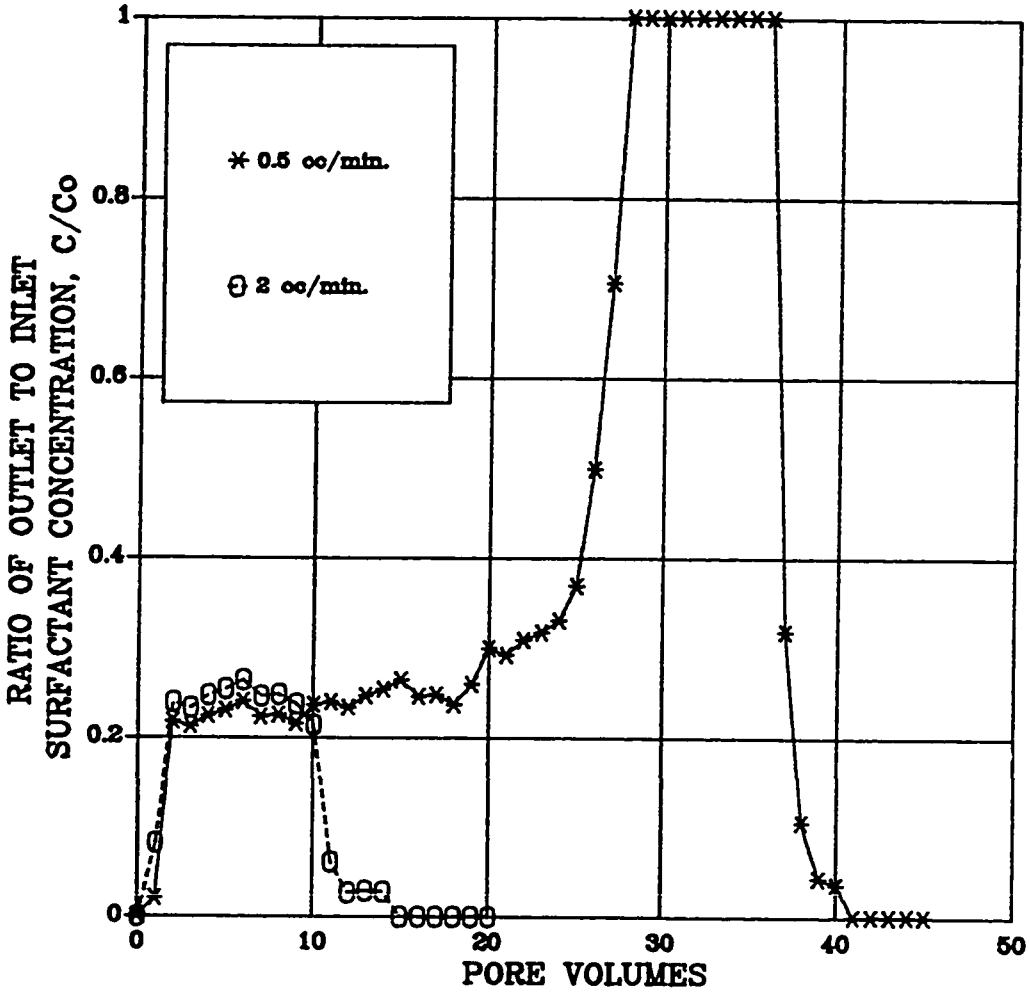

Figure 4.21 Adsorption and desorption profiles of B1083 at a concentration of 0.5%, 57000 ppm, 107 °C, and different flow rates.

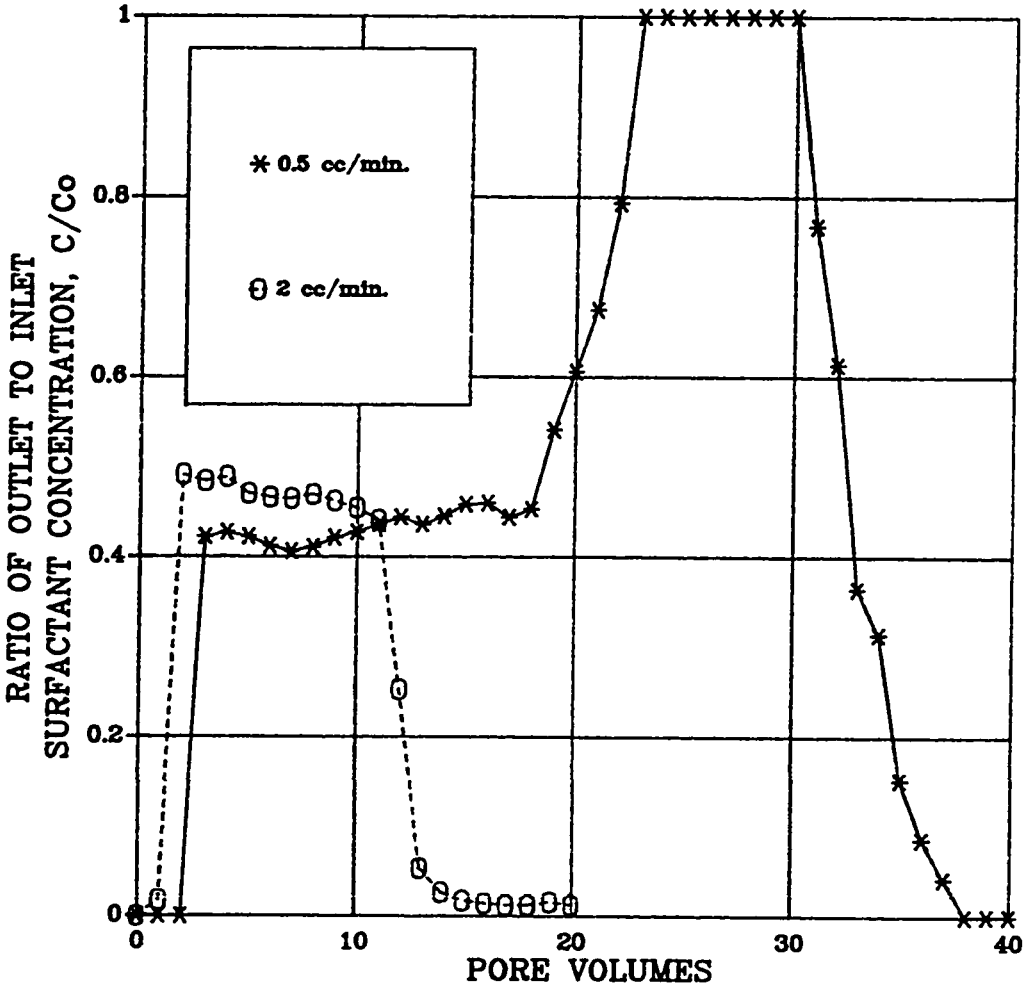

Figure 4.22 Adsorption and desorption profiles of B1083 at a concentration of 1 %, 57000 ppm, 107 °C, and different flow rates.

a plateau for B1083 and Sapogenat T-100.

During the desorption period, the effluent concentration of the nonionic surfactants was still at measurable levels even after injecting ten pore volumes of brine. The anionic surfactant B1083 has shown the lowest desorption level at concentrations below 1 %. The anionic surfactant was desorbed at a rate similar to those found for the nonionics. It is to be noted that the rate of desorption varies more rapidly than the rate of adsorption.

4.3.2 Dynamic adsorption isotherms

The adsorption isotherms for the dynamic tests conducted in the present study for the surfactants show a langmuir type isotherm as seen in Figure 4.23 and Table B.19.

The adsorption of B1083 and Sapogenat T-100 increases sharply as the concentration increases. In spite of having different number of molecules of ethylene oxide which makes up the hydrophilic portion of the surfactant molecule, these two surfactants exhibit similar adsorption isotherms. The nonionic surfactant, Triton X-102, presented a small increase in adsorption with concentration and reached a nearly constant value at about 0.5%.

A marked difference exists in shape among the isotherms of the nonionic surfactants and the other two surfactants. The basic differences in the adsorption behavior could be due to the differences in the molecular structure

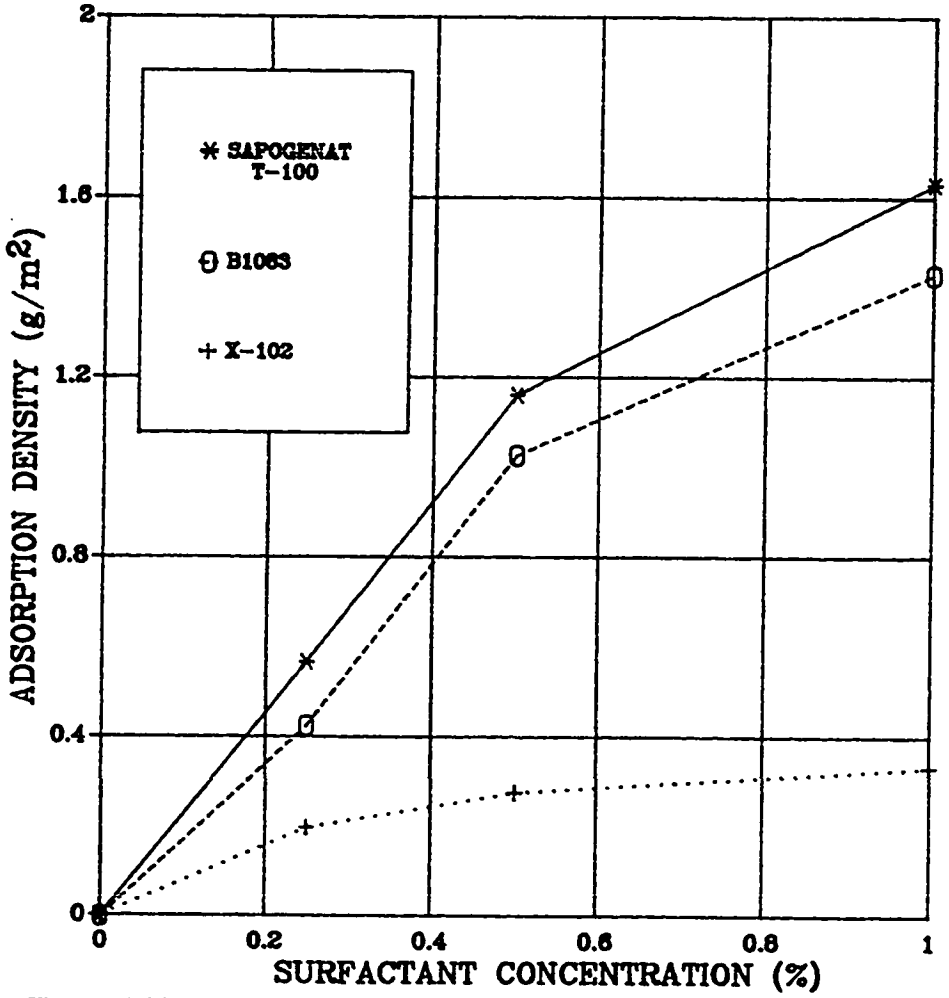

Figure 4.23 Variation of dynamic adsorption density of a carbonate rock with concentration for different types of surfactants at 2 cc/min, 57000 ppm, and 107 °C.

of the different surfactants. Nonionic surfactants differ from anionic and cationic surfactants in that quite small changes in concentration, temperature, or molecular structure of the adsorbate can have a large effect on the adsorption [45].

Corkill et al. [42] studied the adsorption of nonionic surfactants at the graphon solution interface and concluded that the key to understand the adsorption of nonionic surfactants is found in the aqueous solution phase behavior which is often correlated with the cloud point. The cloud point of most nonionic surfactants is a reliable indication of the degree of ethoxylation [42]. In other words, the cloud point increases with increasing the number of molecules of ethylene oxide.

Lewis et al. [44] used ethoxylated alcohol and ethoxylated phenols to minimize the adsorption on Berea core systems and concluded that the cloud point depends on surfactant concentration and brine salinity. He also concluded that the adsorption of a nonionic surfactant can be correlated with temperature and the temperature at which that solution would phase separate. Further studies should be carried out to understand the effect of salinity and temperature on the cloud point of nonionic surfactants used in this study.

Earlier studies [18,19,44] investigated the adsorption of nonionic surfactants on Berea cores and concluded that adsorption of nonionic surfactants is inversely dependent upon extent of ethoxylation. These results

are in agreement with the results presented here for Triton X-102 which has the highest ethoxylation number and presented the lowest adsorption level.

Based on the analysis of the previous results it could be concluded that the nonionic surfactant X-102 exhibited the lowest adsorption, while Sapogenat T-100 presented the highest adsorption.

4.3.3 Desorption isotherms

Figure 4.24 shows a comparison of desorption density for the anionic and nonionic surfactants considered in the dynamic adsorption tests. The desorption density was calculated by taking into account the total amount of surfactant desorbed after injecting several volumes of brine. Figure 4.24 shows that the nonionic surfactants presented a higher desorption level than the anionic surfactant upto a concentration of 1 percent. The Triton X-102 was the one that showed the highest desorption level. A significant change is observed in the slope for concentrations greater than 0.25 %.

It is well known that surfactant retention in porous media is due to the action of several mechanisms such as adsorption, precipitation, and entrapment. Adsorption and entrapment were the main mechanisms responsible for surfactant retention. There is no direct analytical way to determine the relative contribution of the two mechanisms.

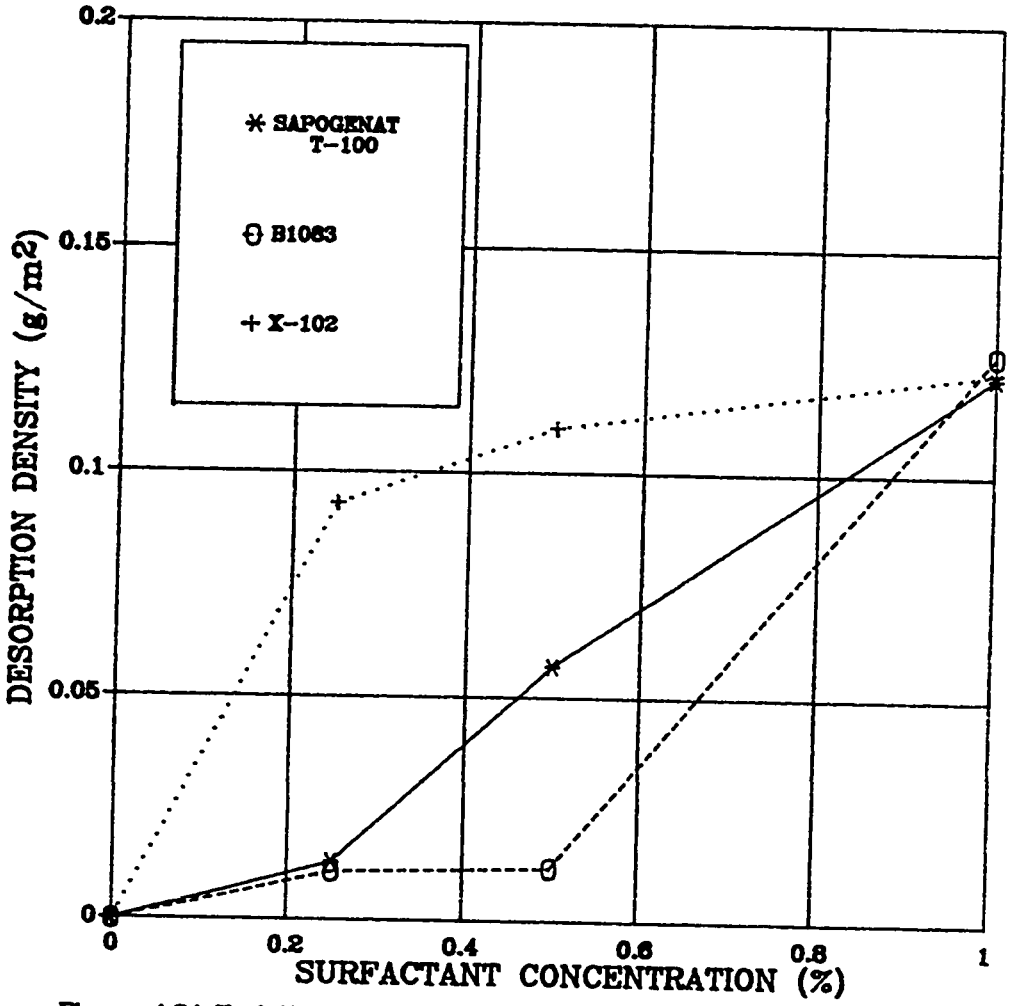

Figure 4.24 Variation of dynamic desorption density of a carbonate rock with concentration for different types of surfactants at 2 cc/min., 57000 ppm, and 107 °C.

It was found that the amount of Triton X-102 recovered from the desorption experiments was more than 30 percent of the amount adsorbed which is desirable for surfactant conservation. Meanwhile, for the other two surfactants less than 5 percent was recovered. This indicates that Triton X-102 is certainly the surfactant with the best performance as far as adsorption and desorption is concerned under these test conditions.

4.4 COMPARISON OF ZETA POTENTIAL AND ADSORPTION ISOTHERMS

The interaction of brine with the solid surface and the nature of the interaction between the surfactant and the solid of the carbonate rock were analyzed through the zeta potential studies. Other important factors such as rate of adsorption, the shape of the adsorption isotherms and the effect of temperature and brine composition were analyzed through the dynamic and static adsorption studies. The next step is to compare the zeta potential to adsorption results in order to find out if the zeta potential can be used to delineate the mechanism of adsorption of surfactants.

Before starting the discussion , it should be noted that the the zeta potential measurements and the adsorption tests were performed at different conditions of temperature and salinity due to the fact that the upper limit of the zeta meter unit is 25000 ppm and it is only possible to make measurements at room temperature. Additionally, the zeta potential procedure has the

drawback of performing the zeta potential measurements in a suspended solution which has to be either deionized water or brine instead of making them directly with the surfactant solution.

4.4.1 Zeta potential and static adsorption isotherms

Figures 4.25 and 4.26 illustrate the comparison of the zeta potential curve and the adsorption isotherms of Triton X-102 and B1083 for static adsorption tests at different salinities and temperatures.

The comparison presented in Figure 4.25 for Triton X-102 indicates no relationship between the adsorption density and the zeta potential.

Figure 4.26 shows that a trend exists between the zeta potential curve and the adsorption isotherms for B1083 at different temperatures and salinities. The adsorption density increases with increasing surfactant concentration, while the zeta potential increases negatively with increasing surfactant concentration upto certain value and then remains constant.

4.4.2 Zeta potential and dynamic adsorption isotherms

Figures 4.27-4.29 show a comparison between the zeta potential and the dynamic adsorption density for Sapogenat T-100, Triton X-102, and B1083 respectively at a pH of 8.0. Since the average pH of the effluents from the dynamic adsorption studies was close to this value the comparison was

restricted to this pH. Figures 4.27 and 4.28 did not indicate any trend between the zeta potential curve and the adsorption density isotherms of Sapogenat T-100 and Triton X-102. The zeta potential curve and the adsorption isotherms for B1083 exhibited similar trends with increase in surfactant concentration, as shows in Figure 4.29.

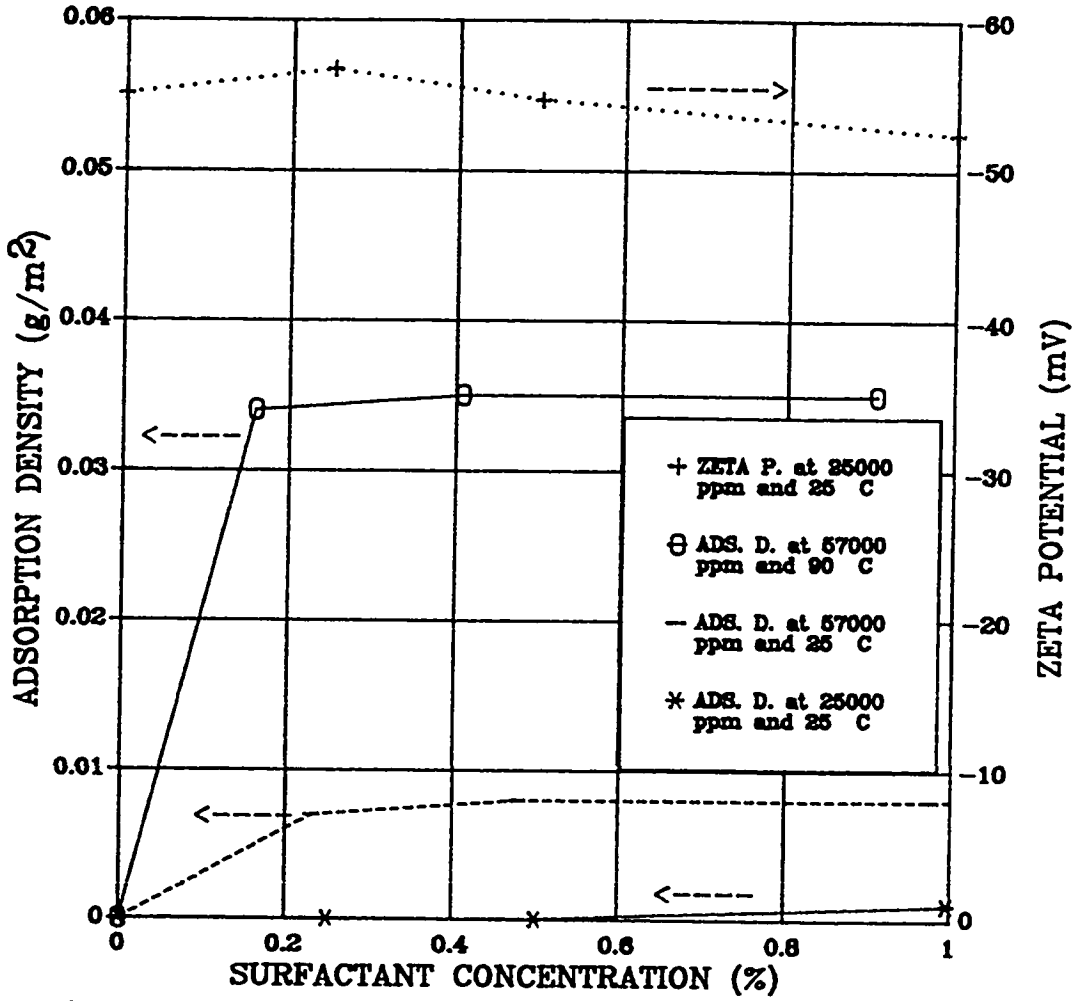

Figure 4.25 Comparison of zeta potential and static adsorption density of a carbonate rock with concentration for Triton X-102 at a pH of 8.0.

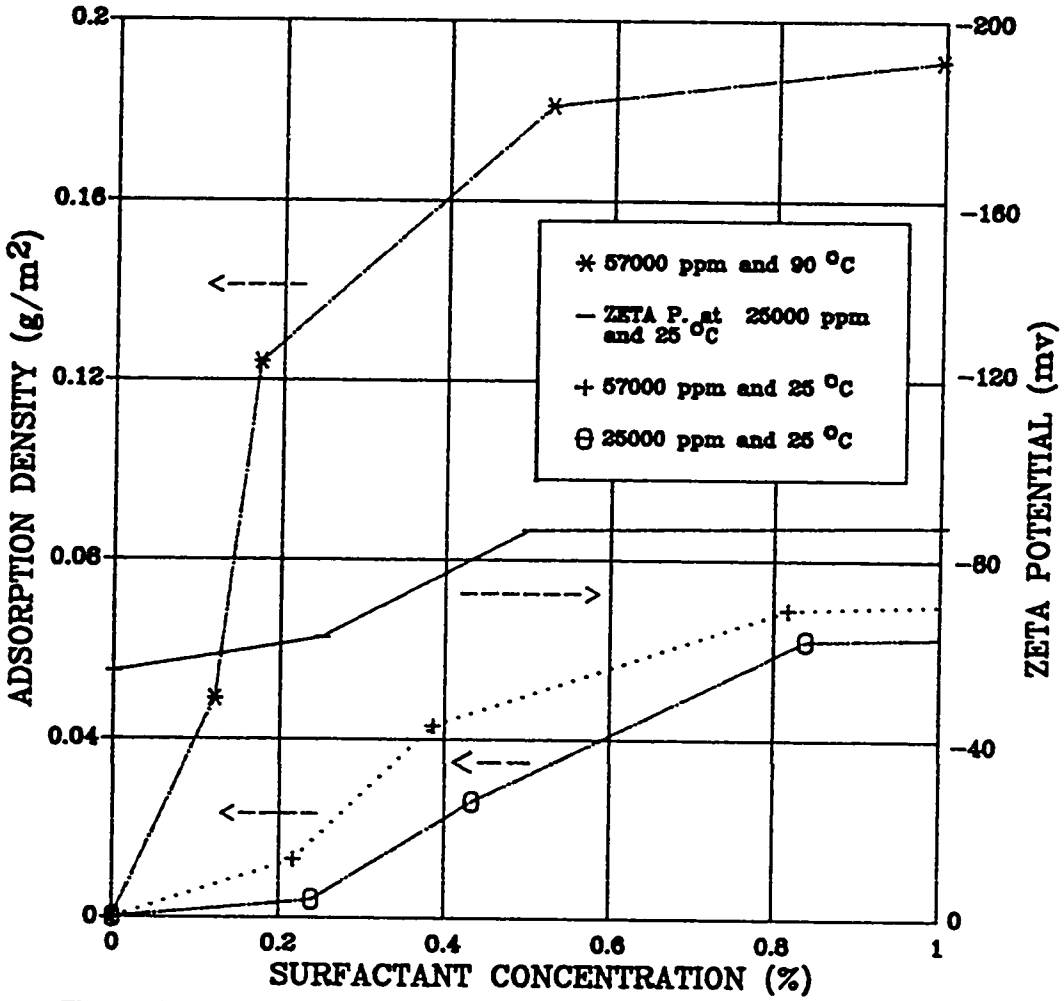

Figure 4.26 Comparison of zeta potential and static adsorption density of a carbonate rock with concentration for BI083 at a pH of 8.0.

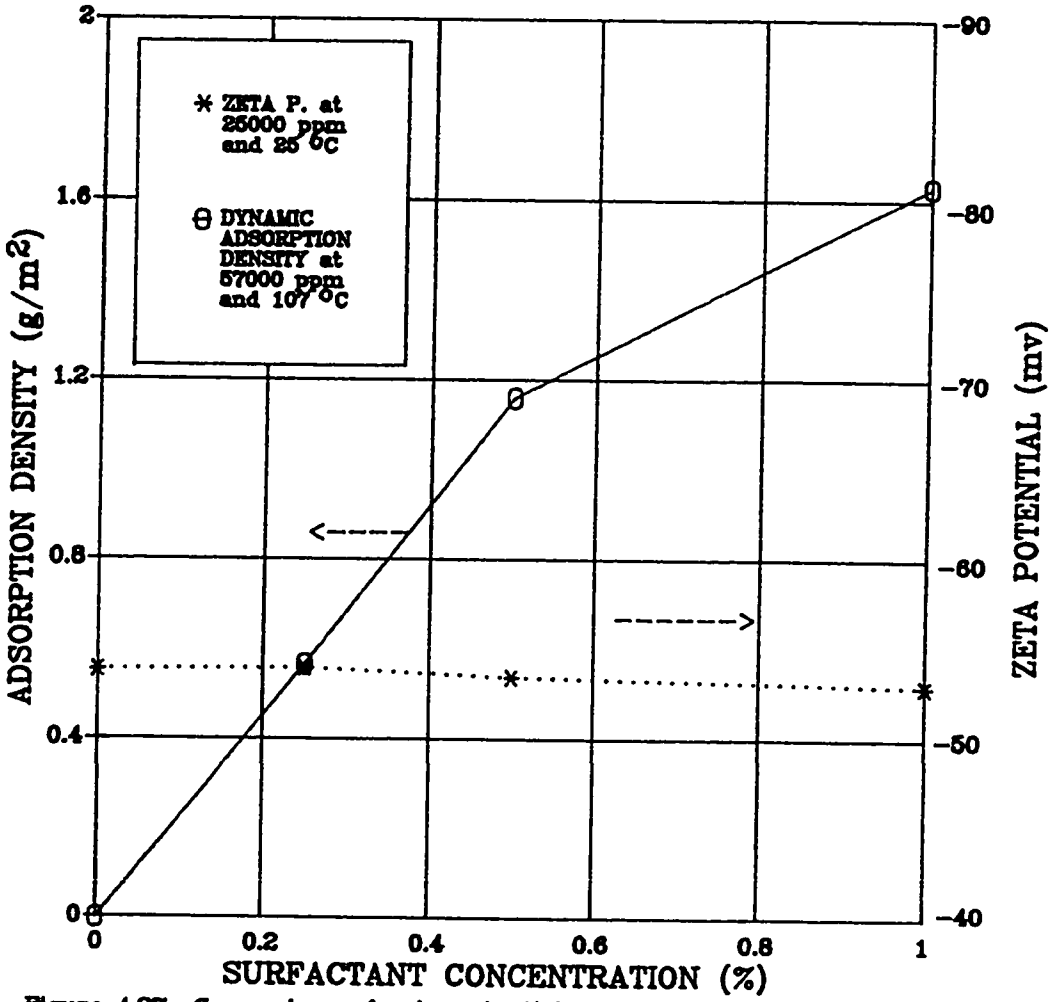

Figure 4.27 Comparison of zeta potential and dynamic adsorption density of a carbonate rock with concentration for Sapogenat T-100 at a pH of 8.0.

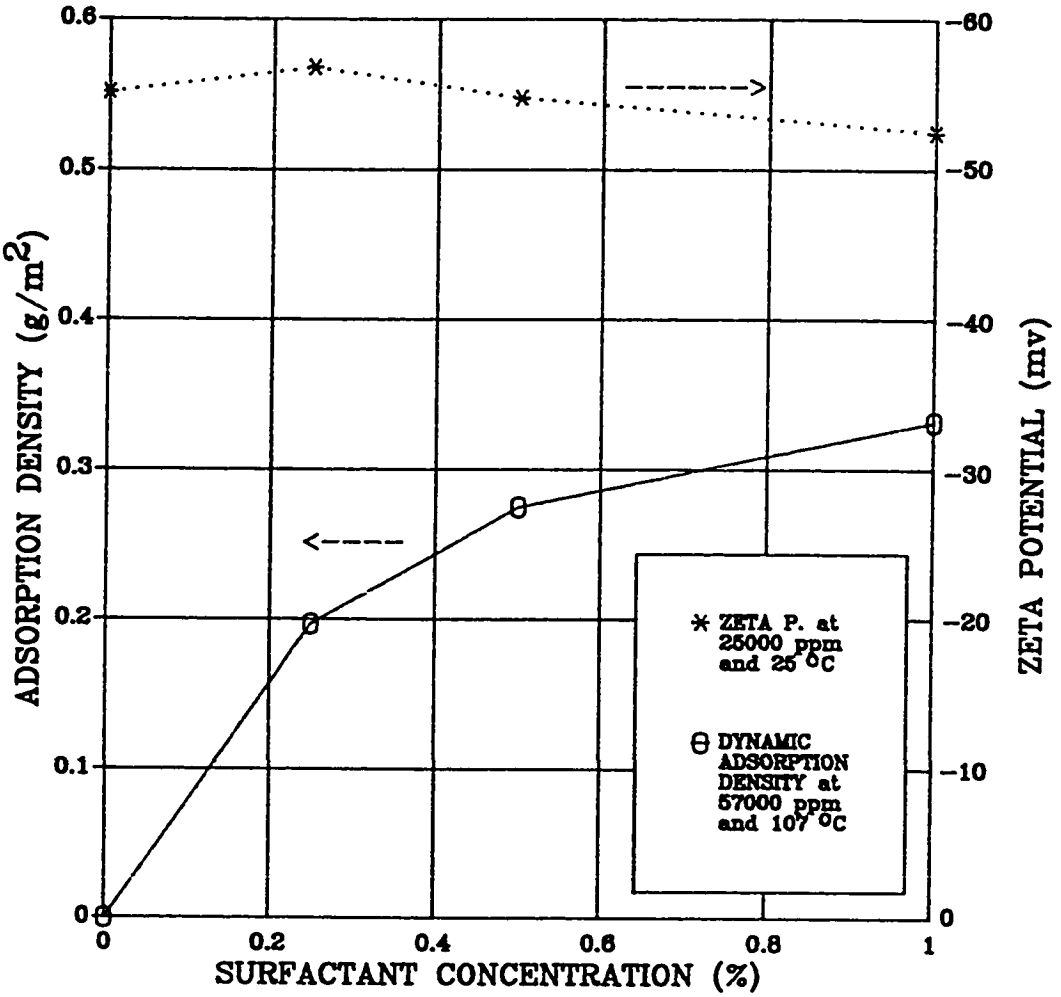

Figure 4.28 Comparison of zeta potential and dynamic adsorption density of a carbonate rock with concentration for Triton X-102 at a pH of 8.0.

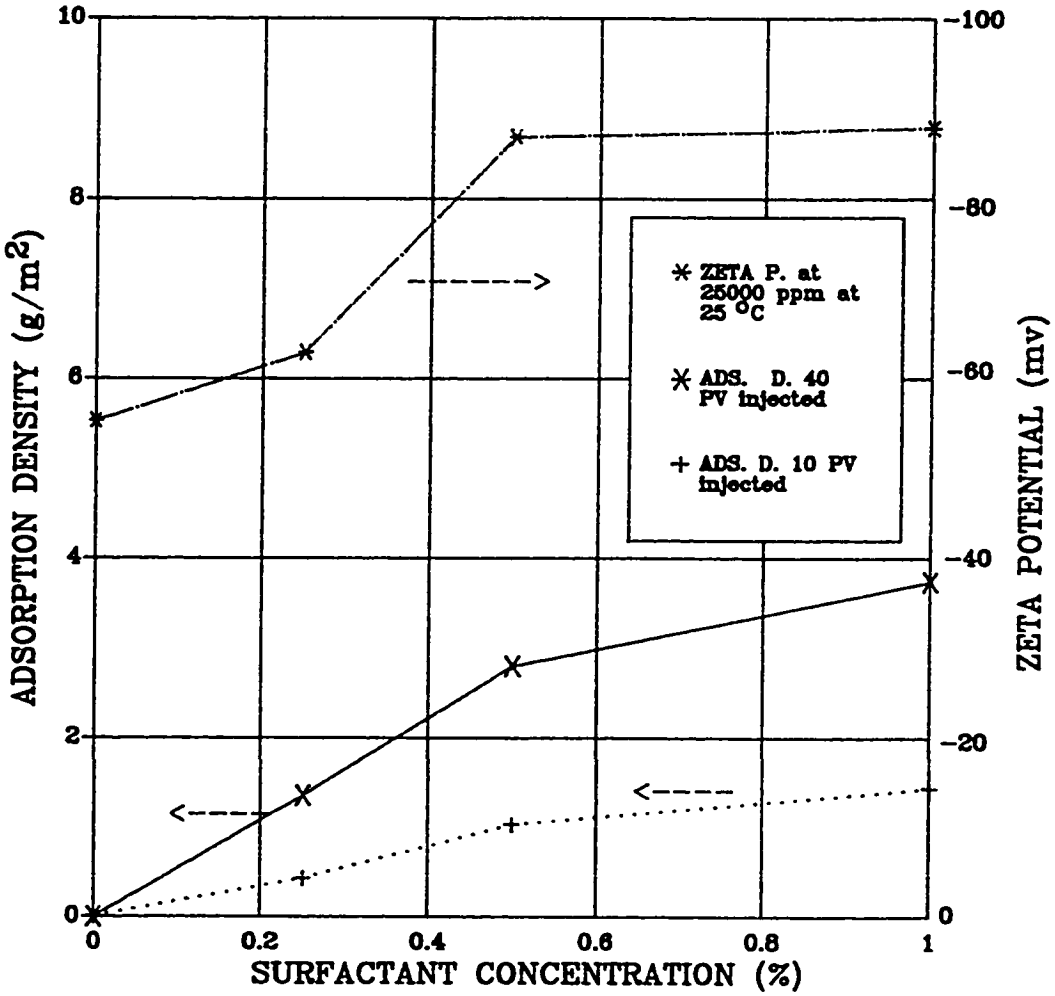

Figure 4.29 Comparison of zeta potential and dynamic adsorption density of a carbonate rock with concentration for B-1083 at a pH of 8.0.

CHAPTER 5

CHAPTER 5

CONCLUSIONS AND RECOMMENDATIONS

5.1 *CONCLUSIONS*

Based on the laboratory investigations and discussions presented in this study, the following conclusions are drawn:

1. The carbonate rock was found to have an isoelectrical point of 4.2 when tested in deionized water, while at high brine salinities the rock surface remained negatively charge over the entire range of pH studied.

2. The nonionic surfactant Triton X-102 presented the lowest adsorption level and the highest desorption level at 107 °C and 57000 ppm TDS. Therefore, as far as adsorption and desorption are concerned, Triton X-102 can be a good candidate to be used in surfactant flooding in carbonate reservoirs.

3. The time required for adsorption equilibrium in dynamic tests varied inversely with the surfactant concentration.

4. The trends obtained from the dynamic adsorption tests correlated very well with the static adsorption experiments.

5. The adsorption isotherms at different salinities and temperatures and the zeta potential curve for the anionic surfactant B1083 showed similar trends.

5.2 *RECOMMENDATIONS*

From the results obtained in this study, the following recommendations are made for the extension of the present work:

1. Interfacial tension studies need be conducted for Triton X-102.

2. A modification of the Zeta meter system should be made to obtain measurements at higher ionic strengths and temperatures.

3. Zeta potential measurements may be used as a potential screening method for adsorption of ionic surfactants. However, more research should be carried out to verify the validity of its use for this purpose.

NOMENCLATURE

NOMENCLATURE

A = Surface area of crushed sample, m^2/g.

A_c = Surface area of rock chips, m^2/g

C/C_o = Ratio of outlet to inlet surfactant concentration.

C_g = A constant related experimentally to the heats of adsorption and liquefaction of the gas.

C_i = Initial surfactant concentration, g/l.

C_o = Average outlet surfactant concentration, g/l

C_r = Residual surfactant concentration, g/l.

P_o = Saturation pressure of adsorbate gas at the experimental temperature.

S = Solid concentration, g/cc.

S_c = Core sample weight, g

TDS = Total dissolved solids.

V = Volume of gas adsorbed at pressure P.

V_i = Volume injected, cc

V_m = Volume of the gas monolayer.

Γ_d = Dynamic adsorption density, g/m^2

Γ_s = Static adsorption density, g/m^2.

REFERENCES

REFERENCES

1. Swisher, R.D. "Surfactant Biodegradation" Surfactant Science Series, vol. 18 (October 1940) 17-19.
2. Mannhardt K., Schramm L.L., and Novosad J.J "Electrokinetic Properties of Reservoir Rock Samples" Colloids and Surfaces , vol. 55 (1991) 309-331.
3. Rosen M.J "Surfactants and Interfacial Phenomena" Wiley-Interscience Publication New York (1978) 26-76.
4. Mannhardt K., Schramm L.L., and Novosad J.J "Effect of Rock Type and Brine Composition on Adsorption of Two Foam-Forming Surfactants", SPE 20463 Presented at 65th Technical Conference of the Soc. of Petroleum Engineers, New Orleans, Sept. 23-26, 1990.
5. Thompson D.W., and Pownall P.M. "Surface Electrical Properties of Calcite" Journal of Colloid and Interfacial Science, vol. 131 (1989) 74-82.
6. Somasundaran P. and Agar G.E. "The Zero Point of Charge of Calcite" Journal of Colloid and Interfacial Science, vol. 24 (1967) 433-440.
7. Lichaa, P.M.,Alpustan, H., Abdul J.H., Nofal W., Al-Hasan Fusseni "Wettability Evaluation of a Carbonate Reservoir Rock", presented at the Third European Core Analysis Symposium, Paris-France Sept. 14-16, 1992.

8. Goujon G. and Mutaftschiev B. "On the Crystallinity and the Stoichiometry of the Calcite Surface" Journal of Colloid and Interfacial Science, vol. 57 (1976) 148-161.

9. Smith A.L. "Electrokinetics of the Oxide- Solution Interface" Journal of Colloid and Interfacial Science, vol. 55 (1976) 526-530.

10. Smallwood P.V. "Some Aspects of the Surface Chemistry of Calcite and Aragonite" Colloid and Polymer Science, vol. 255 (1977) 881-886.

11. Smith R.W. and Shonnard D. "Electrokinetic Study of the Role Modifying Agents in Flotation of Salt-Type Minerals " Journal of Chemical Engineering, vol. 32 (1986) 865-868.

12. Leaist D.G. "Subsurface Dissolution and Precipitation During Leaching of Porous Ionic Solids" Journal of Colloid and Interfacial Science, vol. 118 (1987) 262-269.

13. Sharma M.M, Kuo J.F., and Yen T.F. "Further Investigation of the Surface Charge Properties of Oxide Surface in Oil-Bearing Sands and Sandstones" Journal of Colloid and Interfacial Science, vol. 115 (1987) 9-16.

14. Menezes J.L, Yan J., and Sharma M.M. "The Mechanism of Wettability Alteration Due to Surfactants in Base Muds" SPE 18460 presented at SPE International Symposium on oil field chemistry , Houston, Feb. 8-10,1989.

15. Andersen J.B. and Somasundaran P. "Using Electrophoresis for

Determining the Mechanism of Amine, Sulfate, and Oleate Adsorption on Calcite" Colloid and Surfaces , vol. 55 (1991) 365-368.

16. Trushenki S.P , Douben D.L., and Parrish D.R. "Micellar Flooding , Fluid Propagation, Interaction and Mobility" Journal of Petroleum Technology, (Dec. 1974) 633-645.
17. Bae J.H. and Petrick C.B. "Adsorption of Petroleum Sulfonate in Berea Cores" SPE 5819 presented at SPE-AIME 4th symposium on improved oil recovery , Tulsa, March 22-24, 1976.
18. Novosad J. "Surfactant Retention in Berea Sandstone-Effects of Phase Behavior and Temperature" Society of Petroleum Engineers Journal, (Dec. 1982) 962-970.
19. Celik M.S., Goyal A., Manev A., and Somasundaran P. "The Role of Surfactant in Precipitation and Redissolution in the Adsorption of Sulfonate on Minerals" Journal of Petroleum Technology, (April 1984) 223-239.
20. Hanna H.S., and Somasundaran P. "Physico-chemical Aspects of Adsorption Solid/Liquid Interfaces" Academic press inc. New York city (1977) 337-344.
21. Trogus F. , Schechter R.S., Sophany T., and Wade W.H. "A New Interpretation of Adsorption Maximum and Minimum" Journal of Colloid and Interfacial Science, vol. 70 (1979) 293-305.
22. Trogus F. , Schechter R.S., Sophany T., and Wade W.H. "Static and

Dynamic Adsorption of Anionic and Nonanionic Surfactants" Journal of Petroleum Technology, (Oct. 1977) 337-344.

23. Lawson J.B. "The Adsorption of Non-ionic and Anionic Surfactants on Sandstone and Carbonate" SPE 7052 presented at SPE-AIME 5th symposium on improved methods for oil recovery , Tulsa, April 16-19, 1978.
24. Glover J.C. , Puerto M.C., Maerker J.M., and Sandvick E.L. "Surfactant Phase Behavior and Retention in Porous Media" Journal of Petroleum Technology, (June 1979) 183-193.
25. Smith L., and Malmberg E.W. "The Quantitative Analysis of Adsorbed Petroleum Sulfonate" SPE 5369 presented at SPE-AIME 45th annual California meeting Ventura , April 2-4, 1975.
26. Smith L., and Malmberg E.W. "Measurements of Surfactant Loss in Porous Media" SPE 5306 presented at SPE International Symposium on oil field chemistry , Dallas , Jan. 16-17, 1975.
27. Lawson J.B. , and Dilgren R.E. "Adsorption of Sodium Aryl Sulfonate on Sandstone" Journal of Petroleum Technology, (Feb. 1978) 75-82.
28. Smith L., and Malmberg E.W. "The Adsorption Loss of Surfactant in Tertiary Recovery System" in Improved oil recovery by surfactant and polymer flooding Academic press, New York City (1977) 275-291.
29. Glinsmann G.R. "Surfactant Flooding with Microemulsions Formed In Situ of Oil Characteristics" SPE 8326 presented at SPE-AIME 54th

annual technical meeting conference and exhibition, Las Vegas, Sept. 23-26, 1979.

30. Boneau D.F, and Clampitet R.L. "A Surfactant System for the Oil-Wet Sandstone of the North Burbank Unit" Journal of Petroleum Technology, (April 1977) 501-506.

31. Hanna H.S., and Somasundaran P. "Surface Active Properties of Certain Micellar Systems for Tertiary Oil Recovery" Paper 239 Presented at the 7th International Surface Active Congress, Moscow, Sept. 12-18, 1976.

32. Figdore P.E "Adsorption of Surfactants on Kaolinite: NaCl versus $CaCl_2$ Salt Effects" Journal of Colloid and Interfacial Science, vol. 87 (1982) 500-517.

33. Shakeel Ahmed "Adsorption of Surfactants on Saudi Arabia Limestone" Master Thesis, King Fahd University of Petroleum and Minerals, Dhahran, Saudi Arabia, Aug. 1987.

34. Al-Hashim H.S., Celik M.S., Oskay M.M , and Al-Yousef H.Y. "Adsorption and Precipitation Behavior of Petroleum Sulfonates from Saudi Arabian Limestone" Journal of Petroleum Science Engineering , vol 1(1988) 335-345.

35. Poirier J.E and Cases J.M. "Anionic Surfactant Adsorption onto Silicate Minerals" Colloid and Surfaces , vol. 55 (1991) 333-345.

36. Xu Q., Vasudevan T.V., and Somasundaran P. "Adsorption of

Anionic-Nonionic and Cationic-Nonionic Surfactant Mixtures on Kaolinite". Journal of Colloid and Interfacial Science, vol. 142 (1991) 528-534.

37. KFUPM/RI (1992). Final Report. Rock Wettability: Restoration for Core Analysis and Effect on Oil Recovery. Prepared for Saudi Aramco by the Petroleum and Gas Technology Division, Research Institute, King Fahd University of Petroleum and Minerals, Dhahran.
38. Van Olphen H. "An introduction to clay colloid chemistry" 2nd editon New York, New York, USA (1977) .
39. Novosad J. "Experimental Study and Interpretation of Surfactant Retention in Porous Media" in Enhanced Oil Recovery (Fayers) Elsevier, New York (1981) 101-121.
40. Myers D. "Surfactant Science and Technology" VCH publishers, (1988) 280.
41. Parfitt G.D. and Rochester C.H. "Adsorption of Small Molecules" in Adsorption from Solution at the Solid/Liquid interface (G.D. Parfitt and C.H. Rochester, Eds) Academic press, London (1983) 105-152.
42. Corkill J., Goodman J.F., and Tate J.R. "Adsorption of Nonionic Surface Active-Agents at the Graphon/ Solution Interface" Journal of Colloid and Interfacial Science, vol. 70 (1979) 293-305.
43. "Surfactant for EOR" Hoechst International Report, Frankfurt December 1983.

December 1983.

44. Lewis S.J. and Verkruyse L and Salter S.J. "Selection of Nonionic Surfactants for Minimized Adsorption and Maximize Solubilization" SPE 14910 presented at SPE-AIME 5th symposium on Enhanced Oil Recovery, Tulsa, April 20-23, 1986.

45. Clunnie J.S. and Ingram B.T. "Adsorption of Nonionic Surfactants" in Adsorption from Solution at the Solid/Liquid interface (G.D. Parfitt and C.H. Rochester, Eds) Academic press, London (1983) 105-152.

APPENDICES

Table A.1 Zeta Potential of a Carbonate Rock with pH Tested in Deionized Water

pH	Zeta Potential mV.
2.635	11.780
3.042	5.943
4.554	- 1.684
6.246	- 6.359
7.761	- 8.414
9.324	- 12.210
10.156	- 14.170

Table A.2 Zeta Potential of a Carbonate Rock with pH Tested in 25000 ppm Preserving Brine

pH	Zeta Potential mV.
2.684	- 37.36
3.182	- 39.82
4.114	- 44.85
5.309	- 49.12
7.485	- 56.83
9.920	- 62.25

Table A.3 Zeta Potential of a Carbonate Rock with pH for 0.25% of Sapogenat T-100 Surfactant Tested in Deionized Water

pH	Zeta Potential mV.
2.507	6.804
3.766	1.960
5.801	- 6.203
7.911	- 7.503
8.810	- 9.859
10.007	- 12.470

Table A.4 Zeta Potential of a Carbonate Rock with pH for 0.50% of Sapogenat T-100 Surfactant Tested in Deionized Water

pH	Zeta Potential mV.
2.628	3.154
3.624	1.773
5.735	- 5.368
7.457	- 6.503
9.535	- 10.060
10.451	- 12.220

Table A.5 Zeta Potential of a Carbonate Rock with pH for 1.0% of Sapogenat T-100 Surfactant Tested in Deionized Water

pH	Zeta Potential mV.
2.790	4.673
4.214	- 0.795
5.319	- 3.988
7.886	- 4.218
8.413	- 4.357
9.177	- 4.749
10.147	- 6.460

Table A.6 Zeta Potential of a Carbonate Rock with pH for 2.5.% of Sapogenat T-100 Surfactant Tested in Deionized Water

pH	Zeta Potential mV.
2.441	5.749
3.413	3.207
4.939	- 1.382
7.230	- 8.625
8.625	- 2.812
9.109	- 3.012
9.926	- 4.610

Table A.7 Zeta Potential of a Carbonate Rock with pH for 4.0% of Sapogenat T-100 Surfactant Tested in Deionized Water

pH	Zeta Potential mV.
3.002	4.187
5.206	3.742
8.536	3.642
9.811	3.125
10.241	2.078

Table A.8 Zeta Potential of a Carbonate Rock with pH for 0.25.% of Triton X-102 Surfactant Tested in Deionized Water

pH	Zeta Potential mV.
2.387	10.410
3.520	4.178
4.844	3.790
6.255	- 6.253
8.682	- 9.410
10.284	- 13.360

Table A.9 Zeta Potential of a Carbonate Rock with pH for 0.5% of Triton X-102 Surfactant Tested in Deionized Water

pH	Zeta Potential mV.
2.978	4.851
4.466	- 2.151
6.734	- 7.187
8.448	- 7.953
10.099	- 12.670

Table A.10 Zeta Potential of a Carbonate Rock with pH for 1.0% of Triton X-102 Surfactant Tested in Deionized Water

pH	Zeta Potential mV.
2.482	4.673
3.249	3.234
4.619	- 3.955
6.535	- 5.208
8.413	- 7.901
10.237	- 11.860

Table A.11 Zeta Potential of a Carbonate Rock with pH for 2.5% of Triton X-102 Surfactant Tested in Deionized Water

pH	Zeta Potential mV.
2.578	4.085
3.393	1.635
4.716	- 2.909
6.223	- 4.578
8.452	- 5.039
10.148	- 10.150

Table A.12 Zeta Potential of a Carbonate Rock with pH for 4.0% of Triton X-102 Surfactant Tested in Deionized Water

pH	Zeta Potential mV.
2.295	3.648
3.210	2.342
4.495	- 0.897
6.869	- 1.840
8.563	- 2.750
10.105	- 3.504

Table A.13 Zeta Potential of a Carbonate Rock with pH for 0.25% of B1083 Surfactant Tested in Deionized Water

pH	Zeta Potential mV.
2.267	16.540
2.852	7.257
4.179	- 4.148
6.001	- 8.953
8.295	- 15.810
9.665	- 18.240

Table A.14 Zeta Potential of a Carbonate Rock with pH for 0.5% of B103 Surfactant Tested in Deionized Water

pH	Zeta Potential mV.
2.334	12.970
2.933	9.406
3.536	- 6.265
5.752	- 12.400
7.977	- 16.479
8.997	- 18.601
9.978	- 22.251

Table A.15 Zeta Potential of a Carbonate Rock with pH for 1.0% of B1083 Surfactant Tested in Deionized Water

pH	Zeta Potential mV.
2.790	8.79
3.652	- 7.66
4.791	- 12.80
6.284	- 16.32
7.318	- 19.47
9.313	- 21.60
9.998	- 22.18

Table A.16 Zeta Potential of a Carbonate Rock with pH for 2.5% of B103 Surfactant Tested in Deionized Water

pH	Zeta Potential mV.
2.597	- 7.39
3.721	- 12.82
5.222	- 15.55
6.857	- 18.64
8.319	20.81
9.532	23.70

Table A.17 Zeta Potential of a Carbonate Rock with pH for 4.0% of B1083 Surfactant Tested in Deionized Water

pH	Zeta Potential mV.
2.595	- 11.85
3.360	- 13.21
4.554	- 14.65
6.011	- 17.90
8.575	- 21.78
9.706	- 23.54

Table A.18 Zeta Potential of a Carbonate Rock with pH for 0.25% of Sapogenat T-100 Surfactant Tested in 25000 ppm Preserving Brine

pH	Zeta Potential mV.
2.426	- 38.21
3.650	- 40.87
5.697	- 52.26
7.268	- 56.30
8.251	- 57.91
10.197	- 63.78

Table A.19 Zeta Potential of a Carbonate Rock with pH for 0.5% of Sapogenat T-100 Surfactant Tested in 25000 ppm Preserving Brine

pH	Zeta Potential mV.
2.637	- 35.35
4.250	- 38.33
5.792	- 49.41
7.161	- 54.03
9.239	- 55.32
10.164	- 60.36

Table A.20 Zeta Potential of a Carbonate Rock with pH for 1.0% of Sapogenat T-100 Surfactant Tested in 25000 ppm Preserving Brine

pH	Zeta Potential mV.
2.502	- 36.85
3.536	- 37.40
4.402	- 38.52
6.853	- 51.34
8.325	- 53.56
10.037	- 55.95

Table A.21 Zeta Potential of a Carbonate Rock with pH for 2.5% of Sapogenat T-100 Surfactant Tested in 25000 ppm Preserving Brine

pH	Zeta Potential mV.
2.611	- 36.17
4.996	- 42.52
6.691	- 47.50
8.688	- 51.21
10.247	- 54.56

Table A.22 Zeta Potential of a Carbonate Rock with pH for 4.0% of Sapogenat T-100 Surfactant Tested in 25000 ppm Preserving Brine

pH	Zeta Potential mV.
2.617	- 41.68
4.250	- 40.53
6.885	- 45.46
8.712	- 50.88
10.061	- 53.57

Table A.23 Zeta Potential of a Carbonate Rock with pH for 0.25% of Triton X-102 Surfactant Tested in 25000 ppm Preserving Brine

pH	Zeta Potential mV.
2.387	- 38.21
3.827	- 40.87
6.589	- 56.30
8.734	- 58.67
10.256	- 62.05

Table A.24 Zeta Potential of a Carbonate Rock with pH for 0.5% of Triton X-102 Surfactant Tested in 25000 ppm Preserving Brine

pH	Zeta Potential mV.
2.366	- 39.94
4.096	- 47.79
6.669	- 54.32
8.001	- 56.14
10.229	59.15

Table A.25 Zeta Potential of a Carbonate Rock with pH for 1.0% of Triton X-102 Surfactant Tested in 25000 ppm Preserving Brine

pH	Zeta Potential mV.
2.368	- 36.85
3.953	- 42.40
6.890	- 51.12
8.561	- 55.36
10.920	- 57.95

Table A.26 Zeta Potential of a Carbonate Rock with pH for 2.5% of Triton X-102 Surfactant Tested in 25000 ppm Preserving Brine

pH	Zeta Potential mV.
3.360	- 39.43
5.849	- 48.24
6.947	- 51.98
10.542	- 59.62

Table A.27 Zeta Potential of a Carbonate Rock with pH for 4.0% of Triton X-102 Surfactant Tested in 25000 ppm Preserving Brine

pH	Zeta Potential mV.
2.482	- 40.82
5.102	- 45.55
6.956	- 53.82
9.780	- 62.07

Table A.28 Zeta Potential of a Carbonate Rock with pH for 0.25% of B1083 Surfactant Tested in 25000 ppm Preserving Brine

pH	Zeta Potential mV.
2.292	- 41.40
3.707	- 45.50
5.734	- 51.27
7.152	- 58.01
8.609	64.69
9.491	70.46

Table A.29 Zeta Potential of a Carbonate Rock with pH for 0.5% of B1083 Surfactant Tested in 25000 ppm Preserving Brine

pH	Zeta Potential mV.
2.440	- 40.67
3.777	- 48.65
5.019	- 59.83
6.881	76.57
7.966	- 86.57
8.957	- 90.96
9.919	- 94.63

Table A.30 Zeta Potential of a Carbonate Rock with pH for 1.0% of B1083 Surfactant Tested in 25000 ppm Preserving Brine

pH	Zeta Potential mV.
2.703	- 55.85
3.383	65.28
5.274	- 73.31
7.184	- 89.30
8.635	- 93.40
10.062	- 97.77

Table A.31 Zeta Potential of a Carbonate Rock with pH for 2.5% of B1083 Surfactant Tested in 25000 ppm Preserving Brine

pH	Zeta Potential mV.
2.875	- 63.93
4.183	- 75.96
5.765	- 86.14
7.367	- 102.60
8.982	- 115.10
9.840	- 122.00

Table A.32 Zeta Potential of a Carbonate Rock with pH for 4.0% of B1083 Surfactant Tested in 25000 ppm Preserving Brine

pH	Zeta Potential mV.
2.673	- 62.69
3.330	- 70.89
4.437	- 82.98
5.723	- 94.96
7.202	- 112.50
9.535	- 125.60

Table B.1 Calibration Curve Data for Sapogenat T-100

Concentration (%)	Absorbance
0	0
0.1	0.493
0.2	0.926
0.4	1.416
0.5	1.745

* Wavelength of 500 nm

Table B.2 Calibration Curve Data for B1083

Concentration (%)	Absorbance
0	0
0.1	0.478
0.2	1.542
0.4	2.271
0.5	2.877

* Wavelength of 241.4 nm

Table B.3 Calibration Curve Data for Triton X-102

Concentration (%)	Absorbance
0	0
0.1	0.438
0.2	0.767
0.3	0.971
0.4	1.384
0.5	1.700
0.8	2.282
1.0	2.770
1.5	3.921

* Wavelength of 241.4 nm.

TABLE B.4 Static Adsorption Density Data at 57000 ppm and 90 ℃

SURFACTANT	CONCENTRATION (%)	RESIDUAL CONCENT. (%)	ADSORBED SURFACTANT. (%)	ADSORPTION DENSITY (g/m^2)
B1083	0.25	0.1213	0.1287	0.049
	0.50	0.1726	0.3274	0.124
	1.00	0.5232	0.4768	0.181
	1.50	0.9960	0.5040	0.191
Sapogenat T-100	0.25	0.0097	0.2403	0.091
	0.50	0.0253	0.4747	0.180
	1.00	0.4439	0.5561	0.211
	1.50	0.8961	0.6039	0.229
Triton X-102	0.25	0.1603	0.0897	0.034
	0.50	0.4081	0.0919	0.035
	1.00	0.9064	0.0936	0.035

TABLE B.5 Static Adsorption Density Data at 57000 ppm and 25 °C

SURFACTANT	CONCENTRATION (%)	RESIDUAL CONCENT. (%)	ADSORBED SURFACTANT (%)	ADSORPTION DENSITY (g/m^2)
B1083	0.25	0.2164	0.0336	0.013
	0.50	0.3856	0.1144	0.043
	1.00	0.8167	0.1833	0.069
	2.00	1.801	0.1990	0.075
Triton X-102	0.25	0.2305	0.0195	0.007
	0.50	0.4781	0.0219	0.008
	1.00	0.9762	0.0238	0.009
	2.00	1.9756	0.0244	0.009

TABLE B.6 Static Adsorption Density Data at 25000 ppm and 25 °C

SURFACTANT	CONCENTRATION (%)	RESIDUAL CONCENT. (%)	ADSORBED SURFACTANT (%)	ADSORPTION DENSITY (g/m^2)
B1083	0.25	0.2387	0.0113	0.004
	0.50	0.4323	0.0677	0.026
	1.00	0.8375	0.1625	0.062
	2.00	1.8252	0.1748	0.066
Triton X-102	0.25	0.2500	0.0000	0.000
	0.50	0.5000	0.0000	0.000
	1.00	0.9963	0.0037	0.001
	2.00	1.9953	0.0047	0.002

Table B.7 Effluent Data of Sapogenat T-100 at a Concentration of 0.25% and a Flow Rate of 2 cc/min.

Pore Volumes	Absorbance	Effluent Concentration (%)	Adsorbed Concentration (%)	C/Co
0	0.0	0	0	0
1.0	0.0958	0.0163	0.2337	0.065
2.0	0.0887	0.0150	0.2350	0.060
3.0	0.1005	0.0171	0.2329	0.068
4.0	0.1187	0.0204	0.2296	0.081
5.0	0.1225	0.0210	0.2290	0.084
6.0	0.1373	0.0237	0.2263	0.095
7.0	0.1344	0.0232	0.2268	0.093
8.0	0.1411	0.0224	0.2256	0.098
9.0	0.1378	0.0238	0.2262	0.095
10.0	0.1414	0.0245	0.2255	0.098
11.0 *	0.0658 *	0.0110 *		0.044 *
12.0	0.0586	0.0098		0.0.39
13.0	0.0512	0.0085		0.034
14.0	0.0232	0.0038		0.015
15.0	0.024	0.0039		0.016
16.0	0.0242	0.0040		0.016
17.0	0.0272	0.0045		0.018
18.0	0 .0231	0.0 038		0.015
19.0	0.0226	0.0037		0.015
20.0	0.0037	0.0037		0.015

* Start of desorption process.

Table B.8 Effluent Data of Sapogenat T-100 at a Concentration of 0.5% and a Flow Rate of 2 cc/min.

Pore Volumes	Absorbance	Effluent Concentration (%)	Adsorbed Concentration (%)	C/Co
0	0.0	0	0	0
1.0	0.0475	0.0079	0.4921	0.016
2.0	0.08335	0.0141	0.4859	0.028
3.0	0.1409	0.0244	0.4756	0.049
4.0	0.1814	0.0320	0.4680	0.064
5.0	0.1982	0.0351	0.4649	0.070
6.0	0.1989	0.0353	0.4647	0.071
7.0	0.2001	0.0353	0.4645	0.071
8.0	0.2020	0.0359	0.4641	0.072
9.0	0.2087	0.0372	0.4628	0.074
10.0	0.2040	0.0363	0.4637	0.073
11.0 *	0.1839 *	0.0324 *		0.065 *
12.0	0.1622	0.0283		0.0.57
13.0	0.1491	0.0259		0.052
14.0	0.1426	0.0247		0.049
15.0	0.1342	0.0232		0.046
16.0	0.1316	0.0227		0.045
17.0	0.1321	0.0228		0.046
18.0	0 .1251	0.0 215		0.043
19.0	0.1160	0.0199		0.040
20.0	0.1153	0.0197		0.039

* Start of desorption process.

Table B.9 Effluent Data of Sapogenat T-100 at a Concentration of 1.0% and a Flow Rate of 2 cc/min.

Pore Volumes	Absorbance	Effluent Concentration (%)	Adsorbed Concentration (%)	C/Co
0	0.0	0	0	0
1.0	0.1989	0.0353	0.9647	0.035
2.0	0.6227	0.1301	0.8699	0.0130
3.0	0.7735	0.1702	0.8298	0.170
4.0	1.0733	0.2601	0.7399	0.260
5.0	1.2664	0.3250	0.6750	0.325
6.0	1.4002	0.3733	0.6267	0.373
7.0	1.5623	0.4353	0.5647	0.435
8.0	1.6232	0.4596	0.5404	0.460
9.0	1.6199	0.4583	0.5417	0.458
10.0	1.6436	0.4679	0.5321	0.468
11.0 *	1.3317 *	0.3482 *		0.348 *
12.0	0.5541	0.1129		0.113
13.0	0.4368	0.0852		0.085
14.0	0.2435	0.0440		0.044
15.0	0.2211	0.0396		0.040
16.0	0.2176	0.0389		0.039
17.0	0.1914	0.0338		0.034
18.0	0.1834	0.0 323		0.032
19.0	0.1726	0.0303		0.030
20.0	0.1642	0.0287		0.029

* Start of desorption process.

Table B.10 Effluent Data of Triton X-102 at a Concentration of 0.25% and a Flow Rate of 2 cc/min.

Pore Volumes	Absorbance	Effluent Concentration (%)	Adsorbed Concentration (%)	C/Co
0	0.0000	0 .0000	0.0000	0 .000
1.0	0.0333	0.0087	0.2413	0.035
2.0	0.0551	0.0144	0.2356	0.058
3.0	0.1983	0.0528	0.1972	0.211
4.0	0.4412	0.1210	0.1290	0.484
5.0	0.6433	0.1806	0.0694	0.723
6.0	0.7199	0.2039	0.0461	0.816
7.0	0.7442	0.2114	0..0386	0.846
8.0	0.7961	0.2275	0.0225	0 .910
9.0	0.8059	0.2306	0.0194	0.922
10.0	0.8454	0.2429	0.0071	0.972
11.0 *	0.5048 *	0.1395 *		0.558 *
12.0	0.4452	0.1221		0.489
13.0	0.3505	0.0951		0.380
14.0	0.1997	0.0532		0.213
15.0	0.0731	0.0192		0.077
16.0	0.0607	0.0159		0.063
17.0	0.0598	0.0157		0.846
18.0	0.0557	0.0146		0.846
19.0	0.0521	0.0136		0.055
20.0	0.0513	0.0134		0.054

* Start of desorption process.

Table B.11 Effluent Data of Triton X-102 at a Concentration of 0.5% and a Flow Rate of 2 cc/min.

Pore Volumes	Absorbance	Effluent Concentration (%)	Adsorbed Concentration (%)	C/C_o
0	0.0000	0 .0000	0.000	0 .000
1.0	0.0431	0.0113	0.4887	0.023
2.0	0.5815	0.1621	0.3379	0.324
3.0	0.6645	0.1871	0.3129	0.374
4.0	1.1299	0.3352	0.1648	0.670
5.0	1.4624	0.4496	0.0504	0.899
6.0	1.4532	0.4463	0.0537	0.893
7.0	1.4221	0.4353	0..0647	0.871
8.0	1.4691	0.4520	0.0480	0 .904
9.0	1.5139	0.4679	0.0321	0.936
10.0	1.5898	0.4953	0.0047	0.992
11.0 *	0.9267 *	0.2688 *		0.538 *
12.0	0.4091	0.1118		0.224
13.0	0.2834	0.0763		0.153
14.0	0.2046	0.0545		0.109
15.0	0.1463	0.0387		0.077
16.0	0.1392	0.0368		0.074
17.0	0.1196	0.0315		0.063
18.0	0.1099	0.0290		0.058
19.0	0.0881	0.0231		0.046
20.0	0.0956	0.0251		0.050

* Start of desorption process.

Table B.12 Effluent Data of Triton X-102 at a Concentration of 1.0% and a Flow Rate of 2 cc/min.

Pore Volumes	Absorbance	Effluent Concentration (%)	Adsorbed Concentration (%)	C/Co
0	0.0000	0 .0000	0.000	0 .000
1.0	0.3758	0.1023	0.8977	0.102
2.0	1.6143	0.5043	0.4957	0.504
3.0	2.0845	0.6830	0.3170	0.683
4.0	2.3311	0.7825	0.2175	0.782
5.0	2.6729	0.9269	0.0731	0.927
6.0	2.7091	0.9426	0.0574	0.943
7.0	2.7165	0.9458	0..0542	0.946
8.0	2.7500	0.9605	0.0395	0 .961
9.0	2.7600	0.9649	0.0351	0.965
10.0	2.8720	1.0000	0.0000	1.000
11.0 *	2.3410 *	0.7865 *		0.787 *
12.0	0.8039	0.2299		0.230
13.0	0.2646	0.0710		0.071
14.0	0.2014	0.0537		0.054
15.0	0.1623	0.0430		0.043
16.0	0.0711	0.0186		0.019
17.0	0.0678	0.0178		0.018
18.0	0.0584	0.0153		0.015
19.0	0.0598	0.0157		0.016
20.0	0.0469	0.0123		0.012

* Start of desorption process.

Table B.13 Effluent Data of B1083at a Concentration of 0.25% and a Flow Rate of 2 cc/min.

Pore Volumes	Absorbance	Effluent Concentration (%)	Adsorbed Concentration (%)	C/Co
0	0.0000	0 .0000	0.000	0 .000
1.0	0.0196	0.0116	0.2384	0.046
2.0	0.2301	0.0477	0.2023	0.191
3.0	0.5270	0.0987	0.1513	0.395
4.0	0.5330	0.0998	0.1502	0.399
5.0	0.5460	0.1020	0.1480	0.408
6.0	0.5704	0.1062	0.1438	0.425
7.0	0.5223	0.0979	0..1521	0.392
8.0	0.5294	0.0992	0.1508	0 .397
9.0	0.4979	0.0937	0.1563	0.375
10.0	0.4888	0.0922	0.1578	0.369
11.0 *	0.1571 *	0.0352 *		0.141 *
12.0	0.0425	0.0155		0.062
13.0	0.0146	0.0107		0.043
14.0	0.0000	0.0000		0.000
15.0	0.0000	0.0000		0.000
16.0	0.0000	0.0000		0.000
17.0	0.0000	0.0000		0.000
18.0	0.0000	0.0000		0.000
19.0	0.0000	0.0000		0.000
20.0	0.0000	0.0000		0.000

* Start of desorption process.

Table B.14 Effluent Data of B1083 at a Concentration of 0.5% and a Flow Rate of 2 cc/min.

Pore Volumes	Absorbance	Effluent Concentration (%)	Adsorbed Concentration (%)	C/Co
0	0.0000	0 .0000	0.000	0 .000
1.0	0.1849	0.0411	0.4589	0.082
2.0	0.6241	0.1194	0.3806	0.239
3.0	0.6087	0.1167	0.3833	0.233
4.0	0.6457	0.1233	0.3767	0.247
5.0	0.6655	0.1268	0.3732	0.254
6.0	0.6949	0.1320	0.3680	0.264
7.0	0.6428	0.1228	0..3772	0.246
8.0	0.6486	0.1238	0.3762	0 .248
9.0	0.6176	0.1183	0.3817	0.237
10.0	0.5554	0.1072	0.3928	0.214
11.0 *	0.1285 *	0.0303 *		0.061 *
12.0	0.0304	0.0134		0.027
13.0	0.036	0.0144		0.029
14.0	0.0033	0.0139		0.028
15.0	0.0000	0.0000		0.000
16.0	0.0000	0.0000		0.000
17.0	0.0000	0.0000		0.000
18.0	0.0000	0.0000		0.000
19.0	0.0000	0.0000		0.000
20.0	0.0000	0.0000		0.000

* Start of desorption process.

Table B.15 Effluent Data of B1083 at a Concentration of 1.0% and a Flow Rate of 2 cc/min.

Pore Volumes	Absorbance	Effluent Concentration (%)	Adsorbed Concentration (%)	C/Co
0	0.0000	0 .0000	0.000	0 .000
1.0	0.0561	0.0178	0.9822	0.018
2.0	2.8117	0.4916	0.5084	0.492
3.0	2.7706	0.4845	0.5155	0.484
4.0	2.7989	0.4894	0.5106	0.489
5.0	2.6894	0.4705	0.5295	0.470
6.0	2.6645	0.4663	0.5337	0.466
7.0	2.6555	0.4647	0..5353	0.465
8.0	2.6846	0.4697	0.5303	0.470
9.0	2.6422	0.4624	0.5376	0.462
10.0	2.5965	0.4546	0.5454	0.455
11.0 *	2.4298 *	0.4412 *		0.441 *
12.0	1.3715	0.2526		0.253
13.0	0.2651	0.0537		0.054
14.0	0.1087	0.0269		0.027
15.0	0.0554	0.0177		0.018
16.0	0.0379	0.0147		0.015
17.0	0.0255	0.0126		0.013
18.0	0.0261	0.0127		0.013
19.0	0.0468	0.0162		0.016
20.0	0.0291	0.0132		0.013

* Start of desorption process.

Table B.16 Effluent Data of B1083 at a Concentration of 0.25% and a Flow Rate of 0.5 cc/min.

Pore Volumes	Absorbance	Effluent Concentration (%)	Adsorbed Concentration (%)	C/C_o
0	0.0000	0 .0000	0.000	0 .000
1.0	0.0000	0.0000	0.250	0.000
2.0	0.3277	0.0666	0.1834	0.266
3.0	0.3350	0.0679	0.1821	0.272
4.0	0.3395	0.0687	0.1813	0.275
5.0	0.3586	0.0721	0.1779	0.288
6.0	0.3636	0.0730	0.1770	0.292
7.0	0.3345	0.0678	0..1822	0.271
8.0	0.3378	0.0684	0.1816	0.274
9.0	0.3210	0.0654	0.1846	0.262
10.0	0.3558	0.0716	0.1784	0.286
11.0	0.3620	0.0727	0.1773	0.291
12.0	0.3519	0.0709	0.1791	0.284
13.0	0.3749	0.0750	0.1750	0.300
14.0	0.3836	0.0771	0.1729	0.308
15.0	0.4046	0.0803	0.1697	0.321
16.0	0.3726	0.0746	0.1754	0.0.29
17.0	0.3765	0.0753	0.1747	0.301
18.0	0.3575	0.0719	0.1781	0.288
19.0	0.3962	0.0788	0.1712	0.315
20.0	0.4641	0.0909	0.1591	0.364

Table B.16 Effluent Data of B1083 at a Concentration of 0.25% and a Flow Rate of 0.5 cc/min. (Continuation)

Pore Volumes	Absorbance	Effluent Concentration (%)	Adsorbed Concentration (%)	C/Co
21.0	0.4905	0 .0956	0.1544	0 .382
22.0	0.4747	0.0928	0.1572	0.371
23.0	0.5062	0.0984	0.1516	0.394
24.0	0.5152	0.1000	0.1500	0.400
25.0	0.6364	0.1216	0.1284	0.486
26.0	0.7250	0.1374	0.1126	0.550
27.0	0.8485	0.1594	0.0906	0.638
28.0	0.9237	0.1728	0.0772	0.691
29.0	1.0494	0.1952	0.0548	0.781
30.0	1.1577	0.2145	0.0355	0.858
31.0	1.2138	0.2245	0.0255	0.898
32.0	1.2997	0.2398	0.0102	0.959
33.0	1.3485	0.2485	0.0255	0.994
34.0	1.3569	0.2500	0.0000	1.000
35.0	1.3569	0.2500	0.0000	1.000
36.0	1.3569	0.2500	0.0000	1.000
37.0	1.3569	0.2500	0.0000	1.000
38.0	1.3569	0.2500	0.0000	1.000
39.0	1.3569	0.2500	0.0000	1.000
40.0	1.3569	0.2500	0.0000	1.000

Table B.16 Effluent Data of B1083 at a Concentration of 0.25% and a Flow Rate of 0.5 cc/min. (Continuation)

Pore Volumes	Absorbance	Effluent Concentration (%)	Adsorbed Concentration (%)	C/Co
41.0 *	1.3569 *	0 .2500 *		1.000 *
42.0	1.1644	0.2157		0.863
43.0	0.2071	0.0451		0.180
44.0	0.0000	0.0000		0.000
45.0	0.0000	0.0000		0.000
46.0	0.0000	0.0000		0.000
47.0	0.0000	0.0000		0.000
48.0	0.0000	0.0000		0.000
49.0	0.0000	0.0000		0.0000
50.0	0.0000	0.0000		0.000

* Start of desorption process.

Table B.17 Effluent Data of B1083 at a Concentration of 0.5% and a Flow Rate of 0.5 cc/min.

Pore Volumes	Absorbance	Effluent Concentration (%)	Adsorbed Concentration (%)	C/C_o
0	0.0000	0 .0000	0.000	0 .000
1.0	0.0106	0.0101	0.4899	0.020
2.0	0.5639	0.1087	0.3913	0.217
3.0	0.5488	0.1060	0.3940	0.212
4.0	0.5825	0.1120	0.3880	0.224
5.0	0.6004	0.1152	0.3848	0.230
6.0	0.6273	0.1200	0.3800	0.240
7.0	0.5796	0.1115	0..3885	0.223
8.0	0.5852	0.1125	0.3875	0.225
9.0	0.5572	0.1075	0.3925	0.215
10.0	0.6150	0.1178	0.3822	0.236
11.0	0.6251	0.1196	0.3804	0.239
12.0	0.6083	0.1166	0.3834	0.233
13.0	0.6453	0.1232	0.3768	0.246
14.0	0.6649	0.1267	0.3733	0.253
15.0	0.6947	0.1320	0.3680	0.264
16.0	0.6425	0.1227	0.3773	0.245
17.0	0.6481	0.1237	0.3763	0.247
18.0	0.6172	0.1182	0.3818	0.236
19.0	0.6812	0.1296	0.3704	0.259
20.0	0.7929	0.1495	0.3505	0.299

Table B.17 Effluent Data of B1083 at a Concentration of 0.5% and a Flow Rate of 0.5 cc/min. (Continuation)

Pore Volumes	Absorbance	Effluent Concentration (%)	Adsorbed Concentration (%)	C/Co
21.0	0.7721	0.1458	0.3542	0.292
22.0	0.8187	0.1541	0.3459	0.308
23.0	0.8428	0.1584	0.3416	0.317
24.0	0.8799	0.1650	0.3350	0.330
25.0	0.9876	0.1842	0.3158	0.368
26.0	1.3524	0.2492	0.2508	0.498
27.0	1.9337	0.3528	0.1472	0.706
28.0	2.862	0.5000	0.0000	1.000
29.0	2.8620	0.5000	0.0000	1.000
30.0	2.8620	0.5000	0.0000	1.000
31.0	2.8620	0.5000	0.0000	1.000
32.0	2.8620	0.5000	0.0000	1.000
33.0	2.8620	0.5000	0.0000	1.000
34.0	2.8620	0.5000	0.0000	1.000
35.0	2.8620	0.5000	0.0000	1.000
36.0 *	2.8620 *	0.5000 *		1.000 *
37.0	0.8439	0.1586		0.317
38.0	0.2491	0.0526		0.105
39.0	0.0746	0.0215		0.043
40.0	0.0544	0.0179		0.036

* Start of desorption process.

Table B.17 Effluent Data of B1083 at a Concentration of 0.5% and a Flow Rate of 0.5 cc/min. (Continuation)

Pore Volumes	Absorbance	Effluent Concentration (%)	Adsorbed Concentration (%)	C/Co
41.0	0.0000	0.0000		0.000
42.0	0.0000	0.0000		0.000
43.0	0.0000	0.0000		0.000
44.0	0.0000	0.0000		0.000
45.0	0.0000	0.0000		0.000

Table B.18 Effluent Data of B1083 at a Concentration of 1.0% and a Flow Rate of 0.5 cc/min.

Pore Volumes	Absorbance	Effluent Concentration (%)	Adsorbed Concentration (%)	C/Co
0	0.0000	0 .0000	0.000	0 .000
1.0	0.0000	0.0000	1.000	0.000
2.0	0.0000	0.0000	1.000	0.000
3.0	1.1816	0.4224	0.5776	0.422
4.0	1.1962	0.4274	0.5726	0.427
5.0	1.1816	0.4224	0.5776	0.422
6.0	1.1512	0.4119	0.5881	0.412
7.0	1.1335	0.4059	0.5941.	0.406
8.0	1.1474	0.4107	0.5893	0.411
9.0	1.1788	0.4214	0.5786	0.421
10.0	1.1962	0.4274	0.5726	0.427
11.0	1.2200	0.4363	0.5637	0.436
12.0	1.2445	0.4440	0.5560	0.444
13.0	1.2208	0.4359	0.5641	0.436
14.0	1.2478	0.4451	0.5549	0.445
15.0	1.2866	0.4585	0.5415	0.458
16.0	1.2900	0.4597	0.5403	0.460
17.0	1.2452	0.4443	0.5557	0.444
18.0	1.2710	0.4531	0.5469	0.453
19.0	1.5272	0.5411	0.4589	0.541
20.0	1.7148	0.6056	0.3944	0.606

Effluent was diluted at 50 %

Table B.18 Effluent Data of B1083 at a Concentration of 1.0% and a Flow Rate of 0.5 cc/min. (Continuation)

Pore Volumes	Absorbance	Effluent Concentration (%)	Adsorbed Concentration (%)	C/Co
21.0	1.9157	0.6746	0.3254	0 .675
22.0	2.2625	0.7938	0.2062	0.794
23.0	2.8626	1.0000.	0.0000	1.000
24.0	2.8626	1.0000.	0.0000	1.000
25.0	2.8626	1.0000.	0.0000	1.000
26.0	2.8620	1.0000.	0.0000	1.000
27.0	2.8620	1.0000.	0.0000	1.000
28.0	2.8620	1.0000.	0.0000	1.000
29.0	2.8620	1.0000.	0.0000	1.000
30.0	2.8620	1.0000.	0.0000	1.000
31.0 *	2.1851 *	0.7672 *		0.767 *
32.0	1.7361	0.6129		0.613
33.0	1.0109	0.3637		0.364
34.0	0.8634	0.3131		0.313
35.0	0.3936	0.1516		0.152
36.0	0.1896	0.0816		0.082
37.0	0.0730	0.0415		0.041
38.0	0.0000	0.0000		0.000
39.0	0.0000	0.0000		0.000
40.0	0.0000	0.0000		0.000

Effluent was diluted at 50%

* Start of desorption process.

TABLE B.19 Dynamic Adsorption and Desorption Density Data at 57000 ppm and 107 °C.

SURFACTANT	CONCENTRATION (%)	FLOW RATE (cc/min)	PORE VOLUMES INJECTED	ADSORPTION DENSITY (g/m^2)	DESORPTION DENSITY (g/m^2)
B1083	0.25	2.0	10	0.426	0.011
		0.5	10	0.413	----
		0.5	40	1.357	0.072
	0.50	2.0	10	1.028	0.012
		0.5	10	0.822	----
		0.5	35	2.798	0.072
	1.00	2.0	10	1.431	0.127
		0.5	10	0.997	----
		0.5	30	3.741	0.701
Sapogenat T-100	0.25	2.0	10	0.567	0.013
	0.50	2.0	10	1.161	0.057
	1.00	2.0	10	1.631	0.123
Triton X-102	0.25	2.0	10	0.197	0.093
	0.50	2.0	10	0.275	0.110
	1.00	2.0	10	0.332	0.123